國立交通大學

生物科技學系

碩士論文

利用人類脫氫表雄甾酮亞硫酸基轉移酵素之序列與

結構比對探討其催化機制與功能

From Sequence and Structure of Human Dehydroepiandrosterone Sulfotransferase to Its Mechanism of Action and Function

研究生：呂陸宜

指導教授：楊裕雄 教授

中華民國九十五年五月

利用人類脫氫表雄甾酮亞硫酸基轉移酵素之序列與結構比對探討其催化機制與功能

From Sequence and Structure of Human Dehydroepiandrosterone Sulfotransferase to Its Mechanism of Action and Function

研 究 生：呂陸宜　　Student: Lu-Yi Lu

指導教授：楊裕雄 教授　　Advisor: Prof. Yuh-Shyong Yang

國立交通大學

生物科技學系

碩 士 論 文

A Thesis
Submitted to Department of Biological Science and Technology
National Chiao Tung University
in Partial Fulfillment of the Requirements
for the Degree of
Master of Science
in
Biologic Science and Technology
May 2006
Hsinchu, Taiwan, Republic of China

中華民國九十五年五月

利用人類脫氫表雄甾酮亞硫酸基轉移酵素之序列與結構比對探討其催化機制與功能

學生: 呂陸宜　　指導教授: 楊裕雄 教授

國立交通大學生物科技學系碩士班

摘要

本研究利用人類脫氫表雄甾酮亞硫酸基轉移酵素之胺基酸序列與已知結晶結構來探討其催化機制與功能。亞硫酸基轉移酵素目前大部分已知為同型二聚體，在生理上主要將生物分子亞硫酸化，進而調控許多生理反應與功能。在此研究中，首先為了要瞭解四級結構對此酵素活性之影響，因而藉由定點突變法製備單體之人類脫氫表雄甾酮亞硫酸基轉移酵素與經由膠體過濾分析，我們成功得到單體的亞硫酸基轉移酵素。並由圓二色偏光光譜法來觀測單體與雙體在二級與三級結構上之差異。另外，利用酵素動力學分析探討其催化機制，受質抑制作用，與受質結合能力分析。此外，藉由熱穩定度與尿素變性分析單體與雙體在構型上的穩定度。另一方面，亞硫酸基轉移酵素有一個共同特徵：受質抑制反應。藉由交叉比對分析其結晶結構之二體與三體錯合物，推測可能調控受質抑制反應與受質位向之胺基酸，進而探討受質抑制反應的起源與機制。在此研究中，我們成功地瞭解受質抑制反應與受質位向之間相關性。此外，利用定點突變法與其進一步分析指出，此胺基酸可能在其他亞硫酸基轉移酵素中之相對位置對於受質抑制反應扮演相類似的調控角色。

From Sequence and Structure of Human Dehydroepiandrosterone Sulfotransferase to Its Mechanism of Action and Function

Student: Lu-Yi Lu Advisor: Prof. Yuh-Shyong Yang

Department of Biological Science and Technology and Institute of Biochemical Engineering, National Chiao Tung University, Hsinchu, Taiwan, ROC

ABSTRACT

In this research we deduce the human dehydroepiandrosterone sulfotransferase (SULT2A1) catalytic mechanism and function by the comparison of its amino acid sequences and spatially resolved crystal structures. Sulfotransferase (SULT), mostly known to be homodimer in solution, belongs to an enzyme family that is responsible for the sulfonation of biomolecules and then the regulation of many biological functions. In order to study the effect of quaternary structure on the activity of the enzyme, SULT2A1 monomer mutant is prepared by site-directed mutagenesis and confirmed by gel filtration. Further, the differences of secondary and tertiary structures between dimer and monomer, respectively, are investigated by circular dichroism spectrum. Enzyme kinetics, substrate inhibition and substrate binding affinity are facilitated to deduce the catalytic mechanism and actions. Thermal inactivation and conformational stabilities of dimer and monomer are also determined by enzyme assay and urea unfolding analysis individually. Another general feature of sulfotransferase is substrate inhibition. Following the analysis of the structures of binary and ternary complexes of sulfotransferase, we are able to elucidate the specific amino acids responsible for substrate inhibition and binding orientations. And then we propose the origin and mechanism of substrate inhibition and uncover the relationship between the substrate inhibition and binding orientations. Site-directed mutagenesis and resulting analysis confirm that the involvement of specific amino acid residue in substrate inhibition may be a general feature in all cytosolic sulfotransferases.

ACKNOWLEDGEMENT

終於熬到了這一刻了！雖然辛苦但也著實令人興奮。回想過去從懵懂的專題生到現在略通一二的碩士畢業生，一路走來真是辛苦啊。回首來時路，要感謝的人真的太多了，首先要感謝我的指導教授楊裕雄老師，也真多虧有老師當初能收留一個完全沒有背景知識的專題生，讓我能勉勵自己要汲取更多的知識。而也是因為老師的指導之下，我的思考訓練才有得以呼吸的空間。更感謝的是老師對我的信任，能容忍我一次又一次的失敗，適時地勉勵與關懷，創造了一個絕佳的實驗環境與氣氛，而使學生的時間與空間能更彈性自由。

此外，也要感謝簡慶德老師，黃鎮剛老師，劉明毅老師能擔任我的碩士班口試委員，對我的論文能提出諸多建議以使其更具完整，其用心與指導，在此感謝萬分。而一路走來，幫助我的人太多了！國家同步輻射中心的陳俊榮老師，殷程學長和弘祥學長，清大資工的唐傳義老師以及盈詮，交大生資的PIKI，中研院人很好的饒博士，清大生科的陳婷學姊，還有熱心的一輔宣同學。真多虧有你們的幫助，使我的實驗過程中能多元豐富且更順利，再次感謝啦～

LEPE的夥伴們啊，也真多虧有了你們，讓我平淡無奇的碩士班生涯中多增添了幾分調味。首先要最最感謝的人，就是當初能從pipetman怎麼用開始教的小木學長。教一個完全沒背景的專題生，這完全就是在考驗您老人家的耐心嘛！但最讓我受惠的，是小木學長的人生觀與中心思想，從他的身上，我學到了更多書本上學不到的東西，值得作為人生的準則去追尋。再來就是超厲害的小羊學長(尬酒尬歌都超強)，感覺實驗到他手上就能完全搞定了，雖然我正式踏進來實驗室時他跟小木學長兩老就雙雙離開了(淚)，但對我在專題生時代的訓練，到現在做實驗的態度與執著上，真的有很深遠的影響！阿後啊，陳平狗，一個當了我六年學長的學長，也真多虧了他的照顧，真的是亦學長亦友，不過我們的感情絕不是幾句話就說得完低，在此就介紹完畢。當然，少不了的還有Rich學長啊，三年下來也吃過他不少的好料啊，不過當然最重要的，除了教我很多人生的道理外，也教了我很多生物資訊的觀念，超級受用，都可以去開班了啊。還有好人降大勾，一個我視為最有潛力的研究生，也多虧了有他一路的幫忙，才能讓我的實驗和生活多

了幾分味道，很期待看到你的表現啊，加油！還有感謝鄉民團暨煮粥宵夜團的大晃(鄉長)，嘉蔚(鄉民代表兼賢慧組組員)，僕僕(麵包超人)，淑婷(人超好兼賢慧組組員)。另外也感謝實驗室的莊博，政哲學長，小米，郁吟學姊(人超好)，惠菁學姊(人超好兼賢慧組組長)，好笑又很勁爆的雞姐(原諒我還是喜歡這麼叫你 :))，人很好的來姐，怡宏學長，很拼很有想法的秉鈞學長，超強的得分王小志(球根本就是他養的)，很有一套的昱樹(兼不是很準的氣象官)。再來就是我視為跟降大勾一樣厲害的美春(加油阿，期待你的表現！)，韋汝，很有喜感的小丸，以及曾經待過LEPE且很照顧我的小羿，對我很好的斌勾，可愛的摳卡，阿法勾(超強，生資的魔人兼達人)，carol，還有短暫相處過的Quillan，以及優秀的專題生們(未來實驗室的新血)，謝謝大家啦！！

最後感謝我的家人，能永遠在我的背後給我一個最安穩的後盾和避風港。感謝爸爸和媽媽的栽培及無怨言的支持，沒有你們我決不可能爬上來這研究所的殿堂。還有哥哥，姐姐，以及小妹的支持，讓我能在求學中無後顧之憂地往前衝！送給大家我在桌前的座右銘：

有磨練才能熟練、有投入才能深入、有付出才能傑出！

共勉之～ <(￣﹀￣)>~b

謝謝大家

LE

May, 2006

CONTENTS **PAGE**

CONTENTS OF TABLES AND FIGURES PAGE

Chapter 1

Chapter 2

Chapter 3

Appendix

Abbreviation and Symbol	Full Name
ε	Absorption (extinction) coefficient
$A_{280\ nm}$	Absorption at 280 nm
$A_{600\ nm}$	Absorption at 600 nm
ADT	Androsterone
CD	Circular dichroism
DHEA	Dehydroepiandrosterone
DTT	Dithiothreitol
EDC	Ethyl (dimethyl aminopropyl) carbodiimide
k_{cat}	Turnover number
K_d	Dissociation constant
kDa	Kilodalton
K_i	Inhibitory constant of substrate inhibition
K_m	Michaelis constant
MALDI-TOF	Matrix-assisted laser desorption ionization time-of-flight
MU	4-methylumbelliferone
MUS	4-methylumbelliferyl sulfate
PAPS	3'-phosphoadenosine 5'-phosphosulfate
PAP	Adenosine 3', 5'-diphosphate
PMSF	Phenylmethylsulfonyl fluoride
p NP	4-nitrophenol
RP-HPLC	Reversed phase high performance liquid chromatography
SDS	Sodium Dodecyl Sulfate
SULT	Sulfotransferase
V_{max}	Maximum velocity

CHAPTER 1 Introduction

1.1 Preface

In the post genomic era, great quantities of sequence information are available and most of them are needed to be interpreted for their functional meanings. For example, as the human genomic project is completed in 2003, approximately 20,000-25,000 genes in human DNA were identified and most of them are either unknown or poorly studied. This is following by structural genomics, a field dedicated to a broad understanding of protein structures and functions in relation to gene sequences. The structure of one or more proteins from each family, for a total of about 10000 protein structures in 10 years, will be determined. With these sequence and structure information available, great opportunities have evolved for us to subsequently elucidate the detailed mechanism of enzyme action.

Sulfonation is a widespread biological reaction. Sulfotransferase that catalyzes the transfer of a sulfuryl group from 3'-phosphoadenosine 5'-phosphosulfate (PAPS) to a substrate acceptor group is responsible for all the known biological sulfonation. Pathological and toxicological evidences indicate that the abnormal sulfonation leads to inflammations, cancers and infectious diseases (1-3). Understanding the enzyme catalytic mechanism is important for drug design and therapeutic strategy consequently. The use of structure-based sequence alignments and three-dimensional quantitative structure-activity relationship (3D-QSAR) techniques were shown to be very useful to screen for the inhibitors as drug targets in high throughput scale (4-5).

In this research we deduce the enzyme catalytic mechanism of human dehydroepiandrosterone sulfotransferase (SULT2A1, DHEA-ST) by the comparison of its amino acid sequences and spatially resolved crystal structures. SULT2A1 mainly catalyzes the sulfonation of various steroids and their derivatives, including hydroxysteroids such as

dehydroepiandrosterone (DHEA), androsterone (ADT), testosterone, estradiol, and many endogenous steroids (6-9). Steroid sulfonation has been recognized as an important process for maintaining steroid hormone levels during their metabolism. In humans, dehydroepiandrosterone sulfate (DHEAS) is the most prevalent steroid precursor, and is one of the major secretory products of both adult and fetal adrenals (10). To know more about the actions of SULT2A1 to convert the DHEA to DHEAS, this research from sequence and structure of SULT2A1 is studied and then the deduced enzyme mechanism is further confirmed by site-directed mutagenesis and enzymatic analysis.

1.2 Sulfotransferase

1.2.1 Sulfonation

It has been known for a long time that sulfonation occurs in a biological system. Baumann first described sulfonate conjugation as a pathway in biotransformation in 1876 (11). However, the biochemistry of sulfotransferase enzyme has not been well characterized until the past three decades. Furthermore, the application of molecular biology technology had made it possible to determine the characteristics of these enzymes, whose substrate specificities, regulation, and evolutionary relationships (12). However, the mechanism by which sulfonation takes place was not examined until after the isolation of the active sulfate donor, 3'-phosphoadenosine 5'-phosphosulfate (PAPS), about 80 years later (13).

Sulfotransferases (SULTs) catalyze the transfer of a sulfuryl group from 3'-phosphoadenosine 5'-phosphosulfate (PAPS), the universal sulfonate donor molecule, to a variety of amine and hydroxyl substrates as nucleophiles in a process originally called sulfonation (**Fig. 1**). There are two classes of sulfotransferases: cytosolic sulfotransferases and membrane-associated sulfotransferases. Cytosolic sulfotransferases sulfonate small endogenous and exogenous compounds, such as drugs, steroid hormones, chemical carcinogens, bile acids, and neurotransmitters (14-19). Membrane-associated sulfotransferases, many of which have been implicated recently in crucial biological processes, sulfonate larger biomolecules, suchas carbohydrates and proteins (20-22).

Because of the biological importance and medical relevance of sulfotransferases, there is intense interest in the exact functions of these enzymes. Much information is available with regard to the structure, substrate specificity, and kinetic mechanism of cytosolic sulfotransferases, but less information is available on the transition-state structure and design of potent and specific inhibitors. The membrane-associated enzymes are not as well understood, particularly because their important roles in biological processes have only

recently been uncovered.

1.2.2 Classification of sulfotransferases

The membrane-associated sulfotransferaes are still without a consistent, universal nomenclature scheme and they are named according to their substrate specificity so far. This nomenclature is clarified as required. On the side of cytosolic sulfotransferases, they had often been named after their substrates. However, since the substrate specificities of different sulfotransferases are overlapping, such names can be misleading. To date 10 or 11 human cytosolic sulfotransferases have been characterized and so far the new nomenclature guidelines were applied to 65 sulfotransferase cDNAs and 18 sulfotransferase genes that were characterized from eukaryotic organisms (23). These sequences were evaluated and named on the basis of encoded amino acid sequence identity. Family members share at least 45% amino acid sequence identity whereas subfamily members are at least 60% identical. cDNAs which encode amino acid sequences of at least 97% identity to each other were assigned identical isoform names (**Fig. 2**).

1.2.3 Substrate specificity of sulfotransferases

Although the sulfotransferase mainly possess PAPS as the universal sulfonate donor molecule, a number of studies have also been conducted on the specificity of the PAPS-binding site (24-25). Moreover, different sulfotransferases exhibit distinct substrate specificity. For example, sulfonation of carbohydrates, peptides, hormones, steroids and neurotransmitters are all catalyzed by different sulfotransferases. However, within a subfamily, sulfotransferase has a broad substrate spectrum for similar substrates. As can be seen in **Table I**, the diverse substrate specificity is catalyzed by different sulfotransferases which own oneself preferred substrate. For example, in SULT1 family, the preferred

substrates of sulfotransferase are simple-phenol compounds, such as *p*-nitrophenol (*p*NP), dopamine, and thyroid. Sulfotransferase in SULT2 family, however, mainly catalyzes hydroxysteroids, such as cholesterol, androsterone, dehydroepiandrosterone, pregnenolone, and estradiol. Each of the two families, SULT1A1 and SULT2A1, contains diverse substrate binding site and a separate but identical PAPS binding site.

1.2.4 Structure of cytosolic sulfotransferase

Sulfotransferases are a single α/β globular protein with a characteristic five-stranded parallel β-sheet and α-helices flank both sides of the sheet (26-27). Sulfotransferases share a similar structural resemblance to the nucleotide kinases with their secondary structures conserved not only in position but also in connectivity (28).

The strand–loop–helix and strand–turn–helix motifs constitute the core PAPS binding site, providing the majority of the enzyme interactions with the PAP molecule. The PSB-loop interacts with the 5'-phosphate of the PAP molecule, whereas helix 6 of the strand–turn– helix unit that runs parallel to the PSB-loop provides interaction with the 3'-phosphate. Not only the structures, but also the amino acid sequences of the phosphate-binding sites are conserved in all sulfotransferases including both the cytosolic and membrane enzymes. (29). Furthermore, although the sulfotransferase enzymes display broad substrate specificity, a given enzyme can often be characterized by a specific substrate. The underlying principle that regulates the characteristic substrate specificity is not well developed. Finally, cytosolic sulfotransferases are generally homodimers in their catalytically active forms in solution. The conserved dimerization motif is found in the cytosolic enzymes (30). Multiple amino acid sequence alignments show that the motif consists of ten residues near the C-terminus and is represented by the consensus sequence KXXXTVXXXE. Structural comparisons and mutagenesis studies were undertaken with mouse SUL T1E1 (a monomer) and human

SULT1E1 (a dimer) in an attempt to identify a common structural motif. It was found that the mutations V269E and V260E converted the homodimers SULT1E1 and SULT2A1, respectively, into monomers.

1.3 Dehydroepiandrosterone (DHEA) and dehydroepiandrosterone 3β-sulfate (DHEAS)

1.3.1 Background

Hormones play a plenty of functions physiologically and the abnormal regulation may force the dysfunction and raise the risk, such as the hormone homeostasis and hormone-related disease or metabolism. In this study, I mainly interested in the study of sexual hormone, such as the estradiol, androsterone, testosterone, and dehydroepisterone. For example, the dehydroepisterone (DHEA) plays the profound role and is the precursor of the sexual hormone.The abnormal regulation may cause the irregular secretory amounts of the other hormone as described above. Dehydroepiandrosterone (DHEA) was isolated in urine in 1934, and DHEA 3β-sulfate (DHEAS) was identified 10 years later (31-32). It took another decade to identify DHEA and DHEAS in peripheral blood (33-34). DHEA is one of the hormones produced by the adrenal glands. After being secreted by the adrenal glands, it circulates in the bloodstream as DHEAS and is converted as needed into other hormones. DHEA and DHEAS are the most abundant steroid hormones in the human bloodstream. DHEA is known to be a precursor to the numerous steroid sex hormones (including estrogen and testosterone), which serve well-known functions. While DHEA levels reach their peak in the early morning hours, DHEAS levels show no diurnal variation. It is also one of the most significant age-related biomarkers, which predictably declines with age in even the healthiest of people. Blood levels are highest in the developing fetus, drop sharply after birth, begin climbing again at age 6 to 8 (a time of rapid growth) to a peak at age 25 to 30 and then decline to about 10% of the peak level by age 80 (**Fig. 3**). Abnormally low levels of DHEA have been reported to be related to a number of diseases, including cancer, diabetes, coronary artery disease, and obesity.

1.3.2 Physiological regulation

Little is known about how DHEA works in the body and it often has different effects in men, premenopausal women, and postmenopausal women (35-36). Supplementation with DHEA-S has resulted in increased levels of testosterone and androstenedione (37). The conversion of DHEA into testosterone may account for the fact that low blood levels of DHEA have been reported in some men with erectile dysfunction. The findings of a double-blind trial using 50 mg supplements of DHEA taken daily for six months suggests that DHEA may improve erectile function in some men (38).

1.3.3 DHEA modulates immunity

A group of elderly men with low DHEA levels who were given 50 mg of DHEA per day for 20 weeks experienced a significant activation of immune function (39). Postmenopausal women have also shown increased immune functioning in just three weeks when given DHEA in double-blind research (40). DHEA also regulates the systemic lupus erythematosus (SLE), an autoimmune disease. It has been linked to abnormalities in sex hormone metabolism (41). Supplementation with very large amounts of DHEA (200 mg per day) improved clinical status and reduced the number of exacerbations of SLE in a double-blind trial (42). A preliminary trial has confirmed the benefit of 50-200 mg per day of DHEA for people with SLE (43).

1.3.4 DHEA and cardiopathy

Some reports have suggested that DHEA might reduce the risk of heart disease, perhaps by lowering cholesterol levels. In fact, higher levels of DHEA and DHEAS have been associated with cardiovascular risk factors in women, including high blood pressure and smoking (44). Moreover, DHEA has also been reported to lower HDL (45).

1.4 Conculsion

DHEA is a multifunctional hormone and plays a plenty of function, such as steroid metabolism, cancer, immunity, and aging or more. The sulfated form of DHEA, DHEAS, is primarily in the adrenals, the liver, and small intestines. However, in blood, most DHEA is found as DHEAS with levels that are about 300 times higher than free DHEA. Orally ingested DHEA is converted to its sulfate when passing through intestines and liver. DHEAS is biologically active only after its sulfate group has been split and it becomes DHEA again. From a practical point measurement of DHEAS is preferable to DHEA as levels are more stable. The conversion between DHEA and DHEAS is regulated by SULT2A1 which preferred substrate is DHEA and the regulation of this enzyme and catalytic mechanism is still far from known. In this study we deduce the enzyme mechanism and function from its amino acid sequence and the solved crystal structure. Herein we analyze the quaternary structure, wild-type homodimer and monomer mutant. The monomer mutant, V260E, sufficiently interfere the hydrophobic dimerization interface and the molecular weight is confirmed by gel filtration. Further the circular dichroism spectrum, enzyme kinetics, substrate binding affinity, and the thermal and conformational stability reveal the difference between dimer and monomer of SULT2A1. Moreover, the comparisons of SULT2A1 structure complex also facilitate us to infer the substrate inhibition mechanism and further identify the regulatory amino acid residues. Experimental results and the multiple structural alignment all indicate that the involvement of this amino acid residue in substrate inhibition may be a general feature in all cytosolic sulfotransferases.

REFERENCES

1. Hemmerich, S., Verdugo, D., and Rath, V. L. (2004) Strategies for drug discovery by targeting sulfation pathways. *Drug Discov. Today* **9**, 967–975
2. Kauffman, F. C. (2004) Sulfonation in pharmacology and toxicology. *Drug Metab. Rev.* **36**, 823–843
3. Pasqualini, J. R. (2004) The selective estrogen enzyme modulators in breast cancer: a review. *Biochim. Biophys. Acta.* **1654**, 123–143
4. Sharma, V., and Duffel, M. W. (2005) A comparative molecular field analysis-based approach to prediction of sulfotransferase catalytic specificity. *Methods Enzymol.* **400**, 249–263
5. Rath, V. L., Verdugo, D., and Hemmerich, S. (2004) Sulfotransferase structural biology and inhibitor discovery. *Drug Discov. Today.* **9**,1003–1011
6. Falany, C. N. (1997) Enzymology of human cytosolic sulfotransferases. *FASEB J.* **11,** 206–216
7. Weinshilboum, R. M., Otterness, D. M., Aksoy, I. A., Wood, T. C., Her, C., and Raftogianis, R. B. (1997) Sulfation and sulfotransferases 1: sulfotransferase molecular biology: cDNAs and genes. *FASEB J.* **11,** 3–14
8. Chen, G., Banoglu, E., and Duffel, M. W. (1996) Influence of substrate structure on the catalytic efficiency of hydroxysteroid sulfotransferase STa in the sulfation of alcohols. *Chem. Res. Toxicol.* **9,** 67–74
9. Kakuta, Y., Pedersen, L. C., Chae, K., Song, W. C., Leblanc, D., London, R., Carter, C. W., and Negishi, M. (1998) Mouse steroid sulfotransferases: substrate specificity and preliminary X-ray crystallographic analysis. *Biochem. Pharmacol.* **55,** 313–317
10. Chang, H. J., Shi, R., Rehse, P., and Lin, S. X. (2004) Identifying androsterone (ADT) as

a cognate substrate for human dehydroepiandrosterone sulfotransferase (DHEA-ST) important for steroid homeostasis: structure of the enzyme-ADT complex. *J. Biol. Chem.* **279,** 2689–2696

11. Baumann, E. (1876) *Ber. Dtsch. Chem. Ges.* pp. 54–58
12. Weinshilboum, R. M., Otterness, D. M., Aksoy, I. A., Wood, T. C., Her, C., and Raftogianis, R. B. (1997) Sulfation and sulfotransferases 1: sulfotransferase molecular biology: cDNAs and genes. *FASEB J.* **11**, 3–14
13. Robbins, P. W., and Lipmann, F. (1956) Identification of enzymatically active sulfate as adenosine-3'-phosphate-5'-phosphatesulfate. *J. Am. Chem. Soc.* **78**, 2652–2653
14. Mulder, G. J., and Jakoby, W. B. (1990) in *Conjugation Reactions in Drug Metabolism* (Mulder, G. J., ed) pp. 107–161, Taylor and Francis, Ltd., London
15. Falany, C., and Roth, J. A. (1993) in *Human Drug Metabolism: From Molecular Biology to Man* (Jeffery, E. H., ed) pp. 101–115, CRC Press, Inc. Boca Raton, FL
16. Weinshilboum, R., and Otterness, D. (1994) in *Conjugation-Deconjugation Reactions in Drug Metabolism and Toxicity* (Kaufmann, F. C., ed) pp. 45–78, Springer-Verlag, Berlin
17. DeBaun, J. R., Miller, E. C., and Miller, J. A. (1970) N-hydroxy-2-acetylaminofluorene sulfotransferase: its probable role in carcinogenesis and in protein-(methion-S-yl) binding in rat liver. *Cancer Res.* **30**, 577–595
18. Glatt, H. (1997) Sulfation and sulfotransferases 4: bioactivation of mutagens via sulfation. *FASEB J.* **11**, 314–321
19. Falany, C. N. (1997) Sulfation and sulfotransferases. Introduction: changing view of sulfation and the cytosolic sulfotransferases. *FASEB J.* **11**, 1–2
20. Habuchi, O. (2000) Diversity and functions of glycosaminoglycan sulfotransferases. *Biochem. Biophys. Acta* **1474**, 115–127
21. Grunwell, J. R., and Bertozzi, C. R. (2002) Carbohydrate sulfotransferases of the

GalNAc/Gal/GlcNAc6ST family. *Biochemistry* **41**, 13117–13126

22. Kehoe, J. W, and Bertozzi, C. R. (2000) Tyrosine sulfation: a modulator of extracellular protein-protein interactions. *Chem. Biol.* **7**, 57–61
23. Blanchard, R. L., Freimuth, R. R., Buck, J., Weinshilboum, R. M., and Coughtrie, M. W. (2004) A proposed nomenclature system for the cytosolic sulfotransferase (SULT) superfamily. *Pharmacogenetics* **14**, 199–211
24. Hsiao, Y. S., and Yang, Y. S. (2002) A single mutation converts the nucleotide specificity of phenol sulfotransferase from PAP to AMP. *Biochemistry* **41**, 12959–12966
25. Lin, E. S., and Yang, Y. S. (2000) Nucleotide binding and sulfation catalyzed by phenol sulfotransferase. *Biochem. Biophys. Res. Commun.* **271**, 818–822
26. Kakuta, Y., Pedersen, L. G., Carter, C. W., Negishi, M., and Pedersen, L. C. (1997) Crystal structure of estrogen sulphotransferase. *Nat. Struct. Biol.* **4**, 904–908
27. Negishi, M., Pedersen, L. G., Petrotchenko, E., Shevtsov, S., Gorokhov, A., Kakuta, Y., and Pedersen, L. C. (2001) Structure and function of sulfotransferases. *Arch. Biochem. Biophys.* **390**, 149–157
28. Bidwell, L. M., McManus, M. E., Gaedigk, A., Kakuta, Y., Negishi, M., Pedersen, L., and Martin, J. L. (1999) Crystal structure of human catecholamine sulfotransferase. *J. Mol. Biol.* **293**, 521-530
29. Dajani, R., Cleasby, A., Neu, M., Wonacott, A. J., Jhoti, H., Hood, A. M., Modi, S., Hersey, A., Taskinen, J., Cooke, R. M., Manchee, G. R., and Coughtrie, M. W. (1999) X-ray crystal structure of human dopamine sulfotransferase, SULT1A3. Molecular modeling and quantitative structure-activity relationship analysis demonstrate a molecular basis for sulfotransferase substrate specificity. *J. Biol. Chem.* **274**, 37862-37868
30. Petrotchenko, V., Pedersen, L. C., Borches, C. H., Tomer, K. B., and Negishi, M. (2001) The dimerization motif of cytosolic sulfotransferases. *FEBS Lett.* **490**, 39–43

31. Butemandt, A., and Dannenbaum, H. (1934) *Z. Physiol. Chem.* **229,** 192–195

32. Munson, P. L., Gallagher, T. F., and Koch, F. C. (1944) *J. Biol. Chem.* **152,** 67–77

33. Baulieu, E. E. (1960) Three sulfate esters of 17-ketosteroids in the plasma of normal subjects and after administration of ACTH. *J. Clin. Endocrinol. Metab.* **20,** 900–904

34. Migeon, C. J., and Plager, J. E. (1954) Identification and isolation of dehydroisoandrosterone from peripheral human plasma. *J. Biol. Chem.* **209,** 767–772

35. Weksler, M. E. (1996) Hormone replacement for men. *Br. Med. J.* **312,** 859–860

36. Ebeling, P., and Koivisto, V. A. (1994) Physiological importance of dehydroepiandrosterone. *Lancet* **343,** 1479–1481

37. Stomati, M., Rubino, S., Spinetti, A., Parrini, D., Luisi, S., Casarosa, E., Petraglia, F., and Genazzani, A. R. (1999) Endocrine, neuroendocrine and behavioral effects of oral dehydroepiandrosterone sulfate supplementation in postmenopausal women. *Gynecol. Endocrinol.* **13,** 15–25

38. Reiter, W. J., Pycha, A., Schatzl, G., Pokorny, A., Gruber, D. M., Huber, J. C., and Marberger, M. (1999) Dehydroepiandrosterone in the treatment of erectile dysfunction: a prospective, double-blind, randomized, placebo-controlled study. *Urology* **53,** 590–595

39. Khorram, O., Vu, L., and Yen, S. S. (1997) Activation of immune function by dehydroepiandrosterone (DHEA) in age-advanced men. *J. Gerontol. A Biol. Sci. Med. Sci.* 52, M1–7

40. Casson, P. R., Andersen, R. N., Herrod, H. G., Stentz, F. B., Straughn, A. B., Abraham, G. E., and Buster, J. E. (1993) Oral dehydroepiandrosterone in physiologic doses modulates immune function in postmenopausal women. *Am. J. Obstet. Gynecol.* 169, 1536–1539

41. Lahita, R. G., Bradlow, H. L., Ginzler, E., Pang, S., and New, M. (1987) Low plasma androgens in women with systemic lupus erythematosus. *Arthritis. Rheum.* **30,** 241–248

42. van Vollenhoven, R. F., Engleman, E. G., and McGuire, J. L. (1995)

Dehydroepiandrosterone in systemic lupus erythematosus. Results of a double-blind, placebo-controlled, randomized clinical trial. *Arthritis. Rheum.* **38,** 1826–1831

43. van Vollenhoven, R. F., Morabito, L. M., Engleman, E. G., and McGuire, J. L. (1998) Treatment of systemic lupus erythematosus with dehydroepiandrosterone: 50 patients treated up to 12 months. *J. Rheumatol.* **25,** 285–289
44. Johannes, C. B., Stellato, R. K., Feldman, H. A., Longcope, C., and McKinlay, J. B. (1999) Relation of dehydroepiandrosterone and dehydroepiandrosterone sulfate with cardiovascular disease risk factors in women: longitudinal results from the Massachusetts Women's Health Study. *J. Clin. Epidemiol.* **52,** 95–103
45. Mortola, J. F., and Yen, S. S. (1990) The effects of oral dehydroepiandrosterone on endocrine-metabolic parameters in postmenopausal women. *J. Clin. Endocrinol. Metab.* **71,** 696–704

Table 1: Substrate specificity of human cytosolic sulfotransferases[a].

SULT	Representative	Km (μM)	Km(PAPS) (μM)
1A1	pNP	1.1	1.0
	2-napthol	200	
	dopamine	130	
	tyramine	6483	
	minoxidol	2800	
	3,3'-T2	0.14	
	T3	29.1	
1A2	pNP	69(HAST-4)	5.5(HAST-4) 0.2(HAST-4v)
		4.1(HAST-4v)	
	dopamine	ND	
1A3	pNP	1024	1.1
	tyramine	35	
	dopamine	3.7	
1B1	pNP	5	1.2
	T4	23	
	T3	ND	
	rT3	141	
	3,3'-T2	51	
1C1	pNP	84	8.8
	dopamine	ND	
	N-OH-2AAF	28.6	
1C2	pNP	75.3	
	dopamine	ND	
	N-OH-2AAF	47.5	
1E1	estradiol	0.025	0.3
	DHEA	4.6	
	androstenediol	3.2	
	pNP	76.6	
2A1	estradiol	2.0	1.6
	DHEA	1.0	
	androstenediol	0.2	
	cholesterol		
2B1a	DHEA	2.3	0.1
	pregnenolone	0.2	
	17α–	0.9	
2B1b	DHEA	4.4	0.1
	pregnenolone	0.6	
	17α-hydroxypregnenolone	1.0	
	cholesterol		

[a] Adapted from Chapman *et al*. (2004) *Angew. Chem. Int. Ed. Engl.* **43**, 3526-3548.

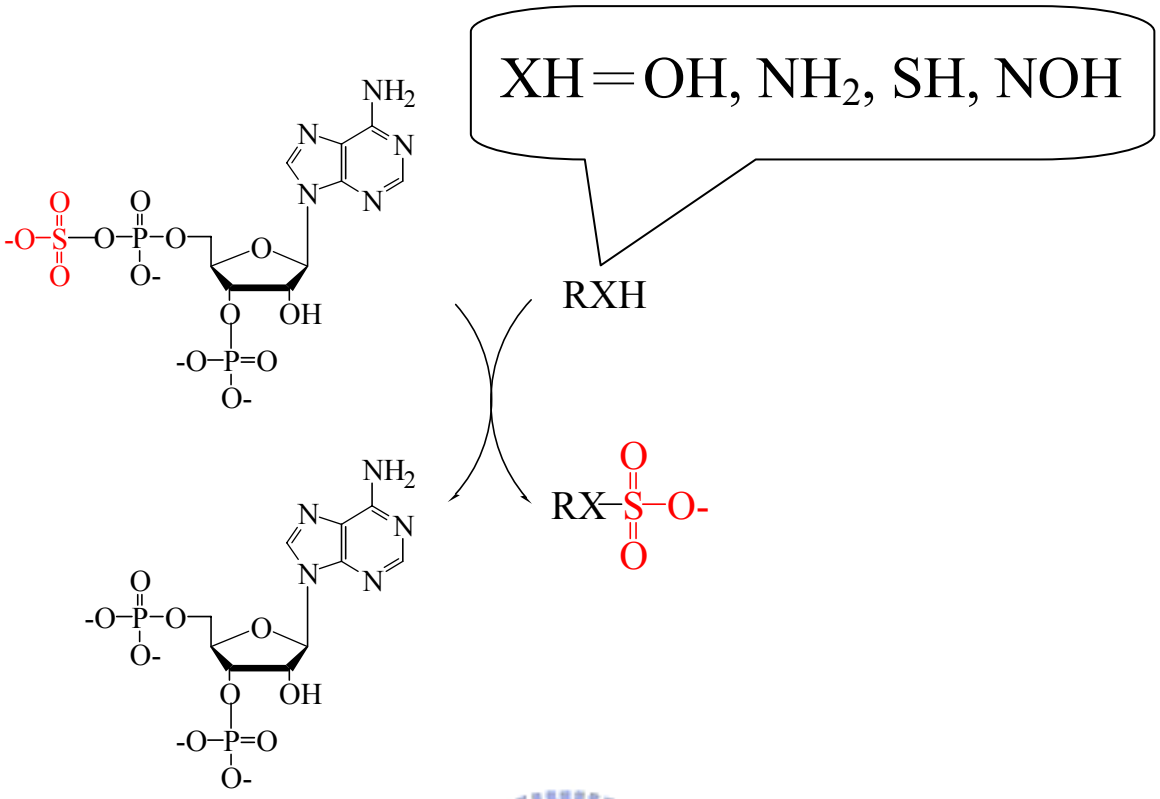

Figure 1. Sulfuryl group transfer in a biological system.

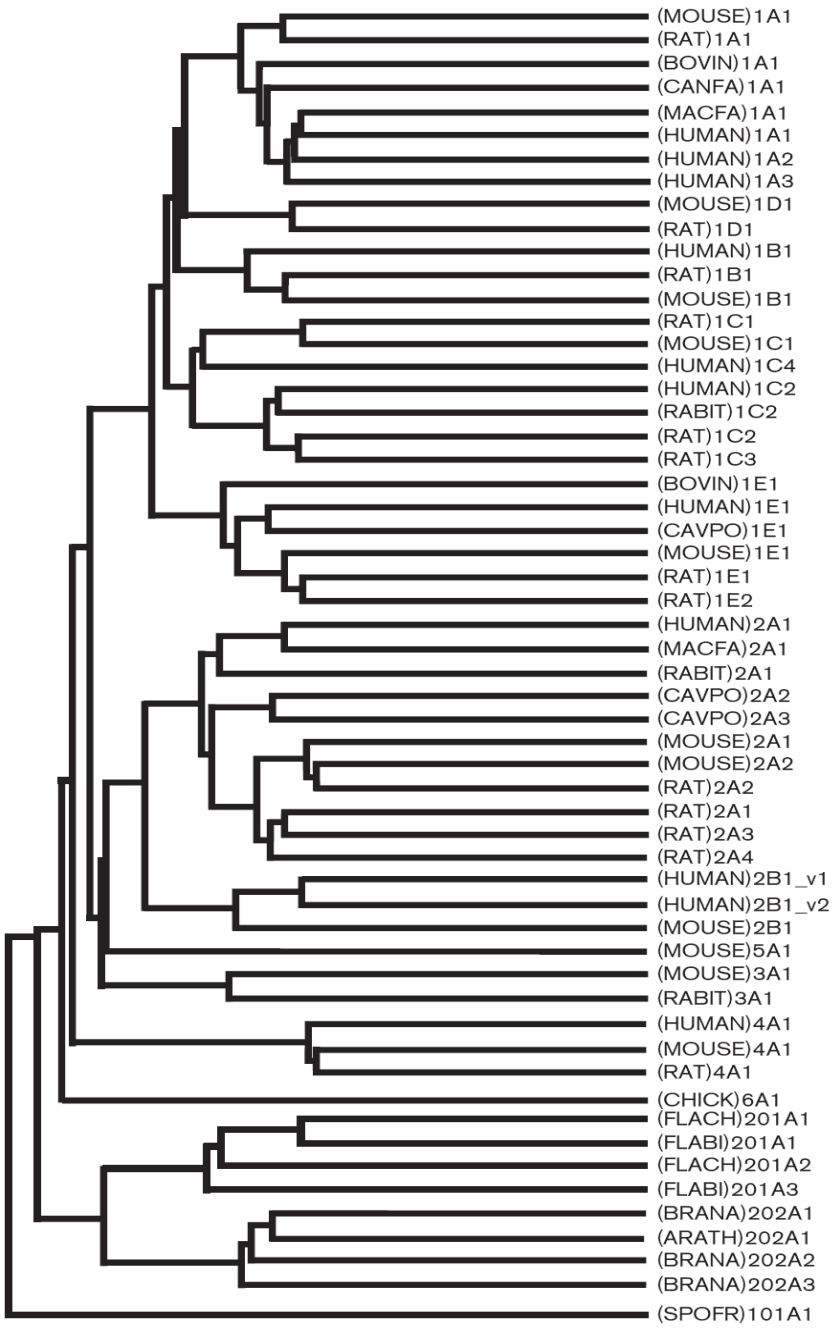

Figure 2. Cytosolic sulfotransferase protein classification on the basis of primary amino acid sequence. The cladogram depicts the evolutionary relationship of sulfotransferase enzyme superfamily members based on their amino acid sequences. (Adapted from Blanchard *et al*. (2004) *Pharmacogenetics.* **14**, 199-211).

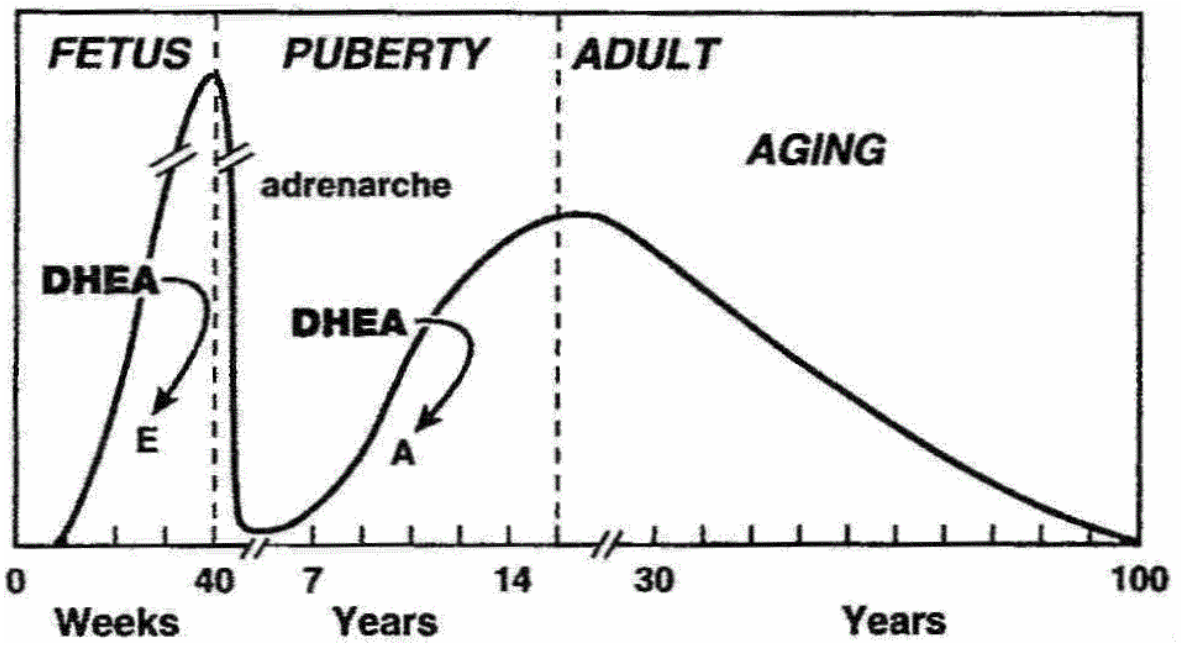

Figure 3. Natural level of DHEA with age. (adapted from the website http://www.benbest.com/).

CHAPTER 2 Effects of Quaternary Structure on the Activity of Human Dehydroepiandrosterone Sulfotransferase

Human dehydroepiandrosterone sulfotransferase (SULT2A1, DHEA-ST) catalyzes the transfer of the sulfuryl group of 3'-phosphoadenosine 5'-phosphosulfate (PAPS) to hydroxysteroids such as dehydroepiandrosterone (DHEA). Most cytosolic sulfotransferases are generally known to be homodimer in solution and the specific amino acid residues responsible for the dimerization have been identified as the KXXXTVXXXE motif (Petrotchenko *et al.* (2001) *FEBS Lett*. 490, 39–43). However, the comparisons of the characteristics and catalytic actions between dimer and monomer of cytosolic sulfotransferases have not been studied in detail so far. To study the effects of quaternary structure on the activity of the enzyme, monomer mutant of SULT2A1 was prepared through site-directed mutagenesis. The mutant V260E of SULT2A1 was sufficient to convert to the monomer by interfering with hydrophobic KTVE motif and confirmed by gel filtration. The circular dichroism spectrum of dimer and monomer mutant reveals the slight conformational change whether in the secondary or tertiary structure. The kinetic constants of dimer and monomer mutant are quite similar whether the PAPS or DHEA are examined, however, the catalytic efficiency, k_{cat}/K_m, shows two folds higher in dimer than that in monomer. It indicates that the two subunits in dimer may be both catalytically competent. The binding affinity shows no significantly change whether for PAP in the binary complex (SULT2A1/PAP) or DHEA in the tertiary complex (SULT2A1/PAP/DHEA) between dimer and monomer. Furthermore, the thermal and conformational stability between dimer and monomer mutant all revealed the monomer is more labile than dimer. The effect of the quaternary structure on SULT2A1 may be a model to deduce the other cytosolic sulfotransferases whether the wild type is the homodimer or monomer in solution naturally.

INTRODUCTION

Sulfotransferases (SULTs) are a large family of enzymes that catalyze the transfer of sulfuryl group from the common 3'-phosphoadenosine 5'-phosphosulfate (PAPS) to numerous endogenous and exogenous compounds. Cytosolic sulfotransferases sulfonate small molecules such as drugs, steroid hormones, chemical carcinogens, bile acids, and neurotransmitters (1-6).

Human dehydroepiandrosterone sulfotransferase (SULT2A1, DHEA-ST) catalyzes the sulfonation of various steroids and their derivatives, including hydroxysteroids such as dehydroepiandrosterone (DHEA), androsterone (ADT), testosterone, estradiol, and many endogenous steroids (7-10). Steroid sulfonation has been recognized as an important process for maintaining steroid hormone levels during their metabolism. In humans, dehydroepiandrosterone sulfate (DHEAS) is the most prevalent steroid precursor, and is one of the major secretory products of both adult and fetal adrenals (11).

Cytosolic sulfotransferases consist of around 300 amino acid residues, and most of them are found as homodimer in solution. Previous study (12) performed the cross-linking by ethyl (dimethyl aminopropyl) carbodiimide (EDC) following the separation by C4 reversed phase high performance liquid chromatography (RP-HPLC) column and analyzed by matrix-assisted laser desorption ionization time-of-flight (MALDI-TOF). It was found that the cross-linked peptides were located between one subunit to the other subunit both nearby the carboxyl terminus, and they also exposured on the surface of each subunit. Therefore the mutants V269E and V260E in human SULT1E1 and SULT2A1, respectively, converted the homodimers into monomers. It was further shown that the mutant P269T and E270V performed simultaneously in mouse SULT1E1, a monomer naturally in solution, forced the formation of the dimer. It was concluded that the general motif KXXXTVXXXE (KTVE

motif) is responsible for the dimerization of cytosolic sulfotransferases.

It had also been reported that sulfotransferases are capable of forming not only homodimers but also the heterodimers (13). Moreover, the crystal structures of numerous cytosolic sulfotransferases have recently been solved and they all contain diverse substrate binding site and a separate but identical PAPS binding site (14-19).

To date, despite the dimerization motif of cytosolic sulfotransferases had been identified (12), the effect of quaternary structure on the catalysis and function of cytosolic sulfotransferases was still far from known and the protein-protein interaction of cytosolic sulfotransferases has not been well studied. The functional significance of the dimerization process is not known at the present time. In this report, we performed that the mutant V260E of SULT2A1 was sufficient to convert the dimer to a monomer by interfering the hydrophobic KTVE motif and confirmed by gel filtration. To investigate the effects of the quaternary structure on the catalysis and function, the studies of the conformational change, catalytic kinetics, substrate inhibition, substrate binding, thermal and conformational stability are all examined. Furthermore the differences between dimer and monomer of SULT2A1 will be clarified and this may be a model to study the effect of quaternary structure among cytosolic sulfotransferases.

EXPERIMENTAL PROCEDURES

Materials—PfuTurbo DNA polymerase was purchased from Stratagene, and MUS, MU, PAP, PAPS, dehydroepiandrosterone (DHEA), glutathione (reduced form), PAP agarose and thrombin were purchased from Sigma (St. Louis, MO). Potassium phosphate (dibasic) was obtained from J. T. Baker (U.S.A.). DEAE Sepharose fast flow, Glutathione S-transferase Sepharose fast flow, Sephacryl S-200 HR, and low molecular weight gel filtration calibration kit were obtained from Amersham Pharmacia Biotech Asia Pacific (Hong Kong). All other chemicals were obtained commercially at the highest purity possible.

Site-Directed Mutagenesis—The QuikChange site-directed mutagenesis kit from Stratagene was used for the generation of monomer mutant of SULT2A1. Briefly, wild-type SULT2A1 cDNA incorporated in pGEX-2TK prokaryotic expression vector was used as the template in conjunction with specific mutagenic primers. The monomer sense mutagenic oligonucleotide primer sets was 5'-tcacttcacagaggcccaagctg-3' for SULT2A1. The amplification conditions were 30 cycles of 30 sec at 95 °C, 1 min at 55 °C, and 7 min at 68 °C. The reaction contained 100 ng of DNA template, 0.4 μM of sense and antisense primers, 200 μM of each of the four deoxynucleotide triphosphates (dNTPs), 1×*Pfu*Turbo buffer, and 2.5 units of *Pfu*Turbo DNA polymerase. The PCR products were treated with DpnI restriction enzyme for 1 hour at 37 °C followed by transforming into DH5α. Mutated cDNA sequences were confirmed using an ABI Prism 377 DNA sequencer (Applied Biosystems, Foster City, CA) following the standard protocol.

Expression, Purification and Characterization of Wild-type and Monomer Mutant of SULT2A1—The expression and purification of SULT2A1 was described previously (20-21). Competent *E. coli* BL21 (DE3) cells transformed with pGEX-2TK vector harboring the wild-type or V260E point-mutated SULT2A1 cDNA were grown to $A_{600\,nm}$ = 0.8 in 0.5 liter

of LB medium supplemented with 50 μg/ml ampicillin. After induction with 1 mM isopropyl β-$_D$-thiogalactopyranoside overnight at 25 ℃, the cells were collected by centrifugation and homogenized in an ice-cold lysis buffer containing 20 mM Tris-HCl, pH 7.5, 150 mM NaCl, 125 mM sucrose, and 10% glycerol using a Fisher Scientific Sonic Dismenbrator. The supernatant collected was fractionated by the glutathione sepharose and the bound fusion protein was treated with 15 units of bovine thrombin for 8 hours at 4 ℃.

A homogeneous protein was obtained as determined by SDS-polyacrylamide gel electrophoresis (22), Protein concentration of the homogeneous form of wild type and monomer mutant SULT2A1 were estimated on the basis of absorbency at 280 nm (2.38 ml/mg cm^{-1}) (23) using a UV/Vis spectrophotometer (Hitachi UV/Vis-3300, Japan).

Size-Exclusion Chromatography and Calibration Curve Preparation—Aliquots of 1ml of various samples was applied on a Sephacryl S-200 HR column that was equilibrated with 20 mM Tris buffer pH 7.5 containing 0.15 M NaCl. Proteins were eluted with the same buffer at a flow rate of 1.0 ml/min. Molecular weights were estimated against calibration standards consisted of ribonuclease A (15.6 kDa), chymotrypsinogen A (19.4 kDa), ovalbumin (47.6 kDa), and albumin (62.9 kDa). Molecular weights of wild type (homodimer) and monomer mutant of SULT2A1 were estimated by gel filtration chromatography (12).

Circular Dichroism Measurement—CD measurements were carried out on a Jasco J715 spectropolarimeter and processed data with J-700 standard analysis version 1.33.00 (Jasco, Japan). CD spectra of enzymes at a concentration of 1 mg/ml in 20 mM phosphate buffer (pH 7.0) were measured in a 1 cm light path length quartz cell in the near-UV range (240-320 nm) and 1 mm light path in the far-UV (200-240 nm) at room temperature.

Enzyme Assay—The activities of wild-type and monomer mutant of SULT2A1 were determined according to the change of fluorescence based on a coupled-enzyme assay method (24). The fluorescence of MU at 460 nm was measured upon excitation at 355 nm. The

reaction mixture with a final volume of 1 ml consisted of 100 mM potassium phosphate buffer at pH 7.0, 5 mM 2-mercaptoethanol, 20 μM PAPS, 2 mM MUS, 5.4 μg K65ER68G (25) of rat SULT1A1, SULT2A1 and 5 μM of DHEA at 37 ℃. A linear response was obtained when 1.49 to 14.9 nM (0.1 to 1 μg) SULT2A1 was added in the standard assay condition (24). In the reaction condition, regeneration of PAPS catalyzed by K65ER68G of rat SULT1A1 is much faster than the production of PAP catalyzed by SULT2A1 for approximately 40 to 50 folds.

Substrate Binding—The dissociation constants (K_d) of PAP and DHEA towards wild-type and monomer mutant of SULT2A1, respectively, were determined with a spectrofluorimeter (26). The decrease in intrinsic fluorescence of protein at 340 nm was observed upon excitation at 280 nm when an aliquot amount of PAP was added into the mixture consisted of 100 mM potassium phosphate buffer at pH 7.0, 100 nM wild-type or monomer mutant of SULT2A1 and varying concentrations of PAP at 25 ℃ with a final volume of 1.3 ml in a quartz cuvette of 1 cm square cross-section. In the ternary experiments, DHEA was added into the pre-incubated solution containing 0.5 μM wild type or monomer mutant of SULT2A1, 100 mM potassium phosphate at pH 7.0, and 1 μM PAP at 25 °C. Each data point was duplicated, and the difference was within 10%.

Thermal Stability—To examine the thermal stability of the wild type and monomer mutant of SULT2A1, aliquots of the protein were treated for 15 minutes at desired temperatures as follows: 25, 30, 35, 40, 45 and 50 °C individually and then were performed by coupled-enzyme assay as described above.

Urea-Dependent Unfolding Experiments—For each data point in the urea denaturation experiment, 5 μM wild type or monomer mutant of SULT2A1 in 20 mM potassium phosphate buffer at pH 7.0 and 10% glycerol was treated at desired concentration of urea from 0 to 6 M at 4 ℃ for approximately 24 hours (27-29). Measurements of circular dichroism at 222 nm

of urea-treated enzymes were made in a Jasco J715 spectropolarimeter at room temperature with a cell of 1 mm path length as described above. CD_{222nm} values were converted into fraction of unfolded values to facilitate comparison of denaturation curves.

Kinetic Data Analysis—Kinetic experiments were analyzed using nonlinear regression to fit the appropriate equation to the data. In non-inhibitory experiments were individually fit to Michaelis-Menten Equation 1, and substrate inhibition data were fitted to substrate inhibition in Equation 2 (30). The kinetic constants (K_m, k_{cat}, and K_i) were obtained from SigmaPlot 2001, V7.0 and Enzyme Kinetics Module, V1.1 (SPSS Inc., Chicago, IL). Data shown represent mean values derived from two determinations.

$$v = V[S]/(K_m + [S]) \qquad \text{(Eq. 1)}$$

$$v = V[S]/\{K_m + [S](1 + [S]/K_i)\} \qquad \text{(Eq. 2)}$$

Analysis of Urea Denaturation Data—This analysis is for a two-state model of denaturation where only the native and the denatured states are populated and it has been found experimentally that the free energy of unfolding of proteins in the presence of denaturant is linearly related to the concentration (27, 31-32). The CD_{222nm} signal, F, plotted as a function of the urea concentration, [Urea], is given by Equation 3, where α is the intercept and β is the slope of the baseline at the native (N) or unfolding (U) state. $[Urea]_{50\%}$ is the urea concentration at the midpoint of urea denaturation, and m value is a constant that is proportional to the increase in the degree of exposure of the protein on denaturation. R is the gas constant, 8.314 J mol^{-1} K^{-1}, and T is the temperature in K. The parameters $\triangle G_{UN}^{H_2O}$, the free energy of denaturation in the absence of urea and is the product of $[Urea]_{50\%}$ and m, and m value were obtained by nonlinear regression fitting of the data to Equation 3 with SigmaPlot 2001, V7.0 and Enzyme Kinetics Module, V1.1 (SPSS Inc., Chicago, IL). The $[Urea]_{50\%}$ is obtained by Equation 4.

$$F = \frac{\{(\alpha_N + \beta_N[\text{Urea}]) + [(\alpha_U + \beta_U[\text{Urea}]) \times \exp[(m[\text{Urea}] - \Delta G_{UN}^{H_2O})/RT]\}}{\{1 + \exp[(m[\text{Urea}] - \Delta G_{UN}^{H_2O})/RT]\}} \quad \text{(Eq. 3)}$$

$$\Delta G_{UN}^{H_2O} = m[\text{Urea}]_{50\%} \quad \text{(Eq. 4)}$$

RESULTS

Enzyme Molecular Weight Estimation—The previous study (12) had shown that the dimerization interface of cytosolic sulfotransferases naturally in solution exists and the subunits form the dimer through the highly conserved sequence KXXXTVXXXE nearby the carboxyl terminus. The KTVE motif of each subunit appears to form a zipper-like and anti-parallel interface, and force the formation of the homodimer consisted of two subunits. The main feature of the interface can be described as the complementary hydrophobic interaction and backbone hydrogen bonds in the central portion of motif that are reinforced by an ion pair at each end of the motif. Accordingly, the mutation V260E of SULT2A1 is produced and then expressed. The molecular weights of wild-type and V260E mutant of SULT2A1 was then estimated by gel filtration. The retention volume (Ve) and the parameter (Kav) were shown as the **TABLE I**. The retention volume of the blue dextran 2000 was 38.1 ml and the Kav could be estimated by the equation: Kav = (Ve – V0) / (Vt – V0). The calibration curve was plotted as the independent variable was log (MW) versus the dependent variable Kav as shown in **Fig. 1**. The retention volume of the wild type and V260E mutant of SULT2A1 was 52.41 and 63.33 ml, respectively (**TABLE II**). The corresponding molecular weight according to the retention volume was shown in **Fig. 1** and the calculated values were approximately equal to the theoretical molecular weight of dimer and monomer of SULT2A1 (**TABLE II**). The estimated molecular weight of wild-type SULT2A1 was approximately 2-fold than that of V260E mutant. These data indicated that the interface of dimerization was easily disrupted through site-directed mutagenesis to force the formation of monomeric SULT2A1 because the glutamic acid might interfere with the hydrophobic zipper-like KTVE motif as similar in previous study (12).

Circular Dichroism Measurement—Analysis by circular dichroism spectrum reveals the

conformational change in dimer and monomer of SULT2A1 whether in the secondary or the tertiary structure. The CD spectrum in the range of far-UV (200-240 nm) (**Fig. 2*A***) indicated the secondary structure showed the slight difference between dimer and monomer in the 205-225 nm, where is the absorption of α-helix and β-sheet. Accordingly, the mutation V260E of SULT2A1, caused the conformational change towards the secondary structure. Furthermore, the tertiary structure of SULT2A1 was also monitored by the CD spectrum in the range of near-UV (240-320 nm) (**Fig. 2*B***). The range in 270-290 nm also revealed the slight difference of tertiary structure because of the absorption of aromatic residue, such as phenylalanine, tyrosine, and tryptophane. The monomer mutant, V260E, caused the environmental change of the α-helixes, β-sheets, and aromatic residues. It may reveal that there is a bit difference between the dimer and monomer although it may affect the whole protein structure or partial quaternary protein structure located near the KTVE motif.

Kinetic Analysis—Rate constants of dimer and V260E mutant of SULT2A1 were shown in **TABLE III**. Either the PAPS or the DHEA was examined in the experiment. K_m for both the dimer and monomer apparently is similar but the catalytic efficiency (k_{cat}/K_m) revealed the dimer was higher than monomer for approximately 2 folds. This result indicated the dimer might competent catalytically in each subunit. Furthermore, the substrate inhibition for DHEA was similar either of the dimer and monomer was examined. These results revealed the each subunit of dimer and the monomer might possess the catalytic ability towards both PAPS and DHEA. The catalytic mechanism, such as the substrate inhibition, is also the same for dimer and monomer of SULT2A1.

Dissociation Constants of PAP and DHEA in Binary and Ternary Complex of Wild-type and V260E Mutant of SULT2A1—So far the crystal structures of cytosolic sulfotransferases all indicate that they all contain the diverse substrate binding site and a separate but identical PAPS binding site (14-19). The dissociative ability of the SULT2A1/PAP complex should be

identical to other cytosolic sulfotransferases. The monomer of SULT2A1, however, was still far from known that the dissociation constants towards the PAPS and DHEA, even the comparison with the dimer of SULT2A1. In this study we performed the dissociation constants of PAP in the binary complex (SULT2A1/PAP) and the DHEA in the ternary complex (SULT2A1/PAP/DHEA) (**TABLE IV**). Whether the dimer or monomer was examined, the K_d values towards PAP in the binary complex and DHEA in the ternary complex revealed no significant differences.

Thermal Stability Dissociation Constants of PAP, DHEA and ADT in Binary and Ternary Dead-end Complex of SULT2A1—Thermal inactivation of SULT2A1 was studied over the temperature range of 25–50 ℃ after the incubation at each desired temperature for 15 min (**Fig. 3**). It was observed that the monomer mutant of SULT2A1 lost only 10% of the basal activity of the control after thermal treatment at 30 ℃ for 15 min. The obvious decreased activities towards dimer and monomer are at the temperature of 40 and 35 ℃, respectively. Also, there is a slight deviation to the previous data reported in the literatures that the tolerance of thermal inactivation was higher at the temperature of 43 ℃ (33) while the dimer of SULT2A1 was examined. It was obvious that the monomer of SULT2A1 was more labile than dimer because the temperature of 50 % thermal inactivation was approximately 35 ℃ for monomer and 40 ℃ for dimer, respectively.

Urea-Dependent Unfolding Experiments—The dimer and monomer of SULT2A1 were examined under the unfolding induction by urea from 0-6 M at 4 ℃ for approximately 24 hours. Typical normalized urea-induction unfolding curves were shown in **Fig. 4** and the data from such transition curves were fitted to Equation 3 and 4 to yield values for $[Urea]_{50\%}$, m value, and $\triangle G_{UN}^{H_2O}$ for dimer and monomer mutant of SULT2A1 (**TABLE V**) (all errors are calculated from the best fit of the data and are not standard deviations from repetitive runs).

Based on these $\triangle G_{UN}^{H_2O}$ values for urea denaturation monitored by CD_{222nm} in **TABLE V**, the thermodynamic stabilities of monomer is more labile than dimer of SULT2A1. Related parameters of urea-induced denaturation are m value, the slope of the transition, and $[Urea]_{50\%}$, the urea concentration at the midpoint of denaturations given in **TABLE V**. The $[Urea]_{50\%}$ was obviously higher in dimer than in monomer mutant.

DISCUSSION

The fact that specific protein-protein interaction can be mediated by short segments of polypeptide chains and it is pivotally important for many physiological processes. For example, upon phosphorylation, ERK2 (a MAP-kinase) forms a homodimer that translocates into the nucleus (this dimerization is mediated by a flexible loop of ERK2 molecule) (34). The key contact surface consists of 12 residues that constitute the hydrophobic zipper-like dimer interface enforced by ion pairs at each end of the zipper (35-36). So far the dimerization interface of cytosolic sulfotransferase had been identified as the KTVE motif (12) and these highly conserved amino acid residues form a zipper-like and anti-parallel interface, and force the formation of the homodimer consisted of two subunits. In this study we mutated the Val-260 to glutamic acid to interfere the hydrophobic interaction and caused the charge-charge repulsion. The V260E mutant of SULT2A1 forces the dissociation of the two subunits of dimer to form the monomer and confirmed by gel filtration as shown in **Fig. 1** and **TABLE II**.

The secondary and tertiary structures reveal slight difference between dimer and monomer by the measurement of circular dichroism spectrum (**Fig. 2**). However, the conformational change may result from the mutation itself because the glutamic acid (negative charge residue) is more hydrophilic than the valine (neutral and more hydrophobic). The site-directed point mutation (V260E) may cause partial conformational change so that there is the slight difference between dimer and monomer. Furthermore, it may also result from the protein-protein interaction between the two subunits of dimer of SULT2A1. Consequently the monomer loses the ability to approach with each other and the secondary and tertiary structure observed by CD spectrum is in fact the true ones without the interference by the other subunit.

The enzyme kinetics reveal the K_m and K_i values are identical whether the dimer or monomer is examined (**TABLE III**). It indicates the catalytic mechanism may be the same even the substrate inhibition reaction. The k_{cat}/K_m, however, is 2 folds higher in dimer than in monomer of SULT2A1. It reveals both the subunits of dimer are competent catalytically and it makes more senses. Moreover, previous study indicated that the binding study with human SULT1E1 (homodimer) is shown that the stoichiometry of PAP or PAPS binding is one ligand with one enzyme (26). It was conflicting that the dimer is half active and the rest one is inactive. Furthermore, the substrate binding study (**TABLE IV**) also reveals that the substrate binding affinity is identical either in PAP or DHEA between dimer and monomer. The each subunit of dimer does not affect the release of the PAP and DHEA, and it could also interpret that the substrate inhibition does not attribute to dimerization of SULT2A1 (37) although the origin of substrate inhibition had been proposed the formation of ternary dead-end complex (26, 38). The K_i values for either of dimer and monomer (**TABLE III**) indicates that substrate inhibition is not the result of dimerization and the release of DHEA does not significantly alter (**TABLE IV**).

Thermal and conformational stability reveal the monomer is more labile and the thermal tolerance is lower than dimer approximately for 5 ℃ while the enzyme activity is inactive for 50 % (**Fig. 3**). The conformational stability examined by urea unfolding experiment shows the monomer is denatured under lower concentration of urea (**Fig. 4**). It may be attributed to the conformational change as described above but it is not clear to know that whether the protein-protein interaction forces the dimer more stable than monomer.

Consequently, we have prepared the monomer of SULT2A1 by site-directed mutagenesis and confirmed by gel filtration. The conformational change, enzyme kinetics, thermal inactivation and conformational stability experiments indicate the monomer and dimer possess slight differences and it is potential to be the model to study the quaternary structure

of cytosolic sulfotransferases and further to pursue the significance and the physiological function.

REFERENCES

1. Mulder, G. J., and Jakoby, W. B. (1990) in *Conjugation Reactions in Drug Metabolism* (Mulder, G. J., ed) pp. 107–161, Taylor and Francis, Ltd., London
2. Falany, C., and Roth, J. A. (1993) in *Human Drug Metabolism: From Molecular Biology to Man* (Jeffery, E. H., ed) pp. 101–115, CRC Press, Inc. Boca Raton, FL
3. Weinshilboum, R., and Otterness, D. (1994) in *Conjugation-Deconjugation Reactions in Drug Metabolism and Toxicity* (Kaufmann, F. C., ed) pp. 45–78, Springer-Verlag, Berlin
4. DeBaun, J. R., Miller, E. C., and Miller, J. A. (1970) N-hydroxy-2-acetylaminofluorene sulfotransferase: its probable role in carcinogenesis and in protein-(methion-S-yl) binding in rat liver. *Cancer Res.* **30,** 577–595
5. Glatt, H. (1997) Sulfation and sulfotransferases 4: bioactivation of mutagens via sulfation. *FASEB J.* **11,** 314–321
6. Falany, C. N. (1997) Sulfation and sulfotransferases. Introduction: changing view of sulfation and the cytosolic sulfotransferases. *FASEB J.* **11,** 1–2
7. Falany, C. N. (1997) Enzymology of human cytosolic sulfotransferases. *FASEB J.* **11,** 206–216
8. Weinshilboum, R. M., Otterness, D. M., Aksoy, I. A., Wood, T. C., Her, C., and Raftogianis, R. B. (1997) Sulfation and sulfotransferases 1: sulfotransferase molecular biology: cDNAs and genes. *FASEB J.* **11,** 3–14
9. Chen, G., Banoglu, E., and Duffel, M. W. (1996) Influence of substrate structure on the catalytic efficiency of hydroxysteroid sulfotransferase STa in the sulfation of alcohols. *Chem. Res. Toxicol.* **9,** 67–74
10. Kakuta, Y., Pedersen, L. C., Chae, K., Song, W. C., Leblanc, D., London, R., Carter, C. W., and Negishi, M. (1998) Mouse steroid sulfotransferases: substrate specificity and

preliminary X-ray crystallographic analysis. *Biochem. Pharmacol.* **55,** 313–317

11. Chang, H. J., Shi, R., Rehse, P., and Lin, S. X. (2004) Identifying androsterone (ADT) as a cognate substrate for human dehydroepiandrosterone sulfotransferase (DHEA-ST) important for steroid homeostasis: structure of the enzyme-ADT complex. *J. Biol. Chem.* **279,** 2689–2696
12. Petrotchenko, E. V., Pedersen, L. C., Borchers, C. H., Tomer, K. B., and Negishi, M. (2001) The dimerization motif of cytosolic sulfotransferases. *FEBS Lett.* **490,** 39–43
13. Kiehlbauch, C. C., Lam, Y. F., and Ringer, D. P. (1995) Homodimeric and heterodimeric aryl sulfotransferases catalyze the sulfuric acid esterification of N-hydroxy-2-acetylaminofluorene. *J. Biol. Chem.* **270,** 18941–18947
14. Gamage, N. U., Duggleby, R. G., Barnett, A. C., Tresillian, M., Latham, C. F., Liyou, N. E., McManus, M. E., and Martin, J. L. (2003) Structure of a human carcinogen-converting enzyme, SULT1A1. Structural and kinetic implications of substrate inhibition. *J. Biol. Chem.* **278,** 7655–7662
15. Lu, J. H., Li, H. T., Liu, M. C., Zhang, J. P., Li, M., An, X. M., and Chang, W. R. (2005) Crystal structure of human sulfotransferase SULT1A3 in complex with dopamine and 3'-phosphoadenosine 5'-phosphate. *Biochem. Biophys. Res. Commun.* **335,** 417–423
16. Kakuta, Y., Pedersen, L. G., Carter, C. W., Negishi, M., and Pedersen, L. C. (1997) Crystal structure of estrogen sulphotransferase. *Nat. Struct. Biol.* **4,** 904–908
17. Shevtsov, S., Petrotchenko, E. V., Pedersen, L. C., and Negishi, M. (2003) Crystallographic analysis of a hydroxylated polychlorinated biphenyl (OH-PCB) bound to the catalytic estrogen binding site of human estrogen sulfotransferase. *Environ. Health Perspect.* **111,** 884–888
18. Rehse, P. H., Zhou, M., and Lin, S. X. (2002) Crystal structure of human dehydroepiandrosterone sulphotransferase in complex with substrate. *Biochem. J.* **364,**

165–171

19. Lee, K. A., Fuda, H., Lee, Y. C., Negishi, M., Strott, C. A., and Pedersen, L. C. (2003) Crystal structure of human cholesterol sulfotransferase (SULT2B1b) in the presence of pregnenolone and 3'-phosphoadenosine 5'-phosphate. Rationale for specificity differences between prototypical SULT2A1 and the SULT2BG1 isoforms. *J. Biol. Chem.* **278,** 44593–44599
20. Chang, H. J., Zhou, M., and Lin, S. X. (2001) Human dehydroepiandrosterone sulfotransferase: purification and characterization of a recombinant protein. *J. Steroid Biochem. Mol. Biol.* **77,** 159–165
21. Sakakibara, Y., Takami, Y., Nakayama, T., Suiko, M., and Liu, M. C. (1998) Localization and functional analysis of the substrate specificity/catalytic domains of human M-form and P-form phenol sulfotransferases. *J. Biol. Chem.* **273,** 6242–6247
22. Laemmli, U. K. (1970) Cleavage of structural proteins during the assembly of the head of bacteriophage T4. *Nature* **227,** 680–685
23. Gill, S. C., and von Hippel, P. H. (1989) Calculation of protein extinction coefficients from amino acid sequence data. *Anal. Biochem.* **182**, 319–326
24. Chen, W. T., Liu, M. C., and Yang, Y. S. (2005) Fluorometric assay for alcohol sulfotransferase. *Anal. Biochem.* **339,** 54–60
25. Yang, Y. S., Marshall, A. D., McPhie, P., Guo, W. X., Xie, X., Chen, X., and Jakoby, W. B. (1996) Two phenol sulfotransferase species from one cDNA: nature of the differences. *Protein Expr. Purif.* **8,** 423–429
26. Zhang, H., Varlamova, O., Vargas, F. M., Falany, C. N., and Leyh, T. S. (1998) Sulfuryl transfer: the catalytic mechanism of human estrogen sulfotransferase. *J. Biol. Chem.* **273,** 10888–10892
27. Jackson, S. E., Moracci, M., elMasry, N., Johnson, C. M., and Fersht, A. R. (1993) Effect

of cavity-creating mutations in the hydrophobic core of chymotrypsin inhibitor 2. *Biochemistry* **32,** 11259–11269

28. Wallace, L. A., Sluis-Cremer, N., and Dirr, H. W. (1998) Equilibrium and kinetic unfolding properties of dimeric human glutathione transferase A1-1. *Biochemistry* **37,** 5320–5328
29. MacDonald, R. I., and Pozharski, E. V. (2001) Free energies of urea and of thermal unfolding show that two tandem repeats of spectrin are thermodynamically more stable than a single repeat. *Biochemistry* **40,** 3974–3984
30. Cornish-Bowden, A. (1995) *Analysis of Enzyme Kinetic Data*, pp. 118–122, Oxford University Press, Oxford
31. Tanford, C. (1968) Protein denaturation. *Adv. Protein Chem.* **23,** 121–282
32. Pace, C. N. (1986) Determination and analysis of urea and guanidine hydrochloride denaturation curves. *Methods Enzymol.* **131,** 266–279
33. Kudlacek, P. E., Clemens, D. L., Halgard, C. M., and Anderson, R. J. (1997) Characterization of recombinant human liver dehydroepiandrosterone sulfotransferase with minoxidil as the substrate. *Biochem. Pharmacol.* **53,** 215–221
34. Khokhlatchev, A. V., Canagarajah, B., Wilsbacher, J., Robinson, M., Atkinson, M., Goldsmith, E., and Cobb, M. H. (1997) Phosphorylation of the MAP kinase ERK2 promotes its homodimerization and nuclear translocation. *Cell* **93,** 605–615
35. Scheufler, C., Brinker, A., Bourenkov, G., Pegoraro, S., Moroder, L., Bartunik, H., Hartl, F. U., and Moarefi, I. (2000) Structure of TPR domain-peptide complexes: critical elements in the assembly of the Hsp70-Hsp90 multichaperone machine. *Cell* **101,** 199–210
36. Cobb, M. H., and Goldsmith, E. J. (2000) Dimerization in MAP-kinase signaling. *Trends Biochem. Sci.* **25,** 7–9
37. Pedersen, L. C., Petrotchenko, E. V., and Negishi, M. (2000) Crystal structure of

SULT2A3, human hydroxysteroid sulfotransferase. *FEBS Lett.* **475,** 61–64

38. Duffel, M. W., and Jakoby, W. B. (1981) On the mechanism of aryl sulfotransferase. *J. Biol. Chem.* **256,** 11123–11127

TABLE I

Calibration curve determination of molecular weight on Sephacryl S-200 HR.

	MW	log(MW)	Ve[a]	Kav[b]
Albumin	67000	4.83	51.77	0.17
Ovabumin	43000	4.63	57.26	0.23
Chymotrypsinofen A	25000	4.40	72.83	0.42
Ribonuclease A	13700	4.14	81.14	0.53

[a] Ve represented the retention volume of eluted protein under the condition as indicated under "Experimental Procedures."

[b] Kav was calculated by the equation: Kav = (Ve – V0) / (Vt – V0). The Vt was the column volume as 120 ml and the V0 was the retention volume of blue dextran 2000 (2000 kDa), whose retention volume was 38.1 ml.

TABLE II

Physical and chemical parameters of wild type and monomer mutant of SULT2A1.

SULT2A1	Molecular weight[a]	Theoretical pI[a]	Ve[b]
Wild type	68994	5.5	52.41
V260E	34541	5.3	63.33

[a] The molecular weight and theoretical isoelectric point (pI) were determined by the ProtParam on the EXPASY server (http://tw.expasy.org/tools/protparam.html).

[b] The Ve indicated the retention volume as described above and determined by Sephacryl S-200 HR.

TABLE III

Rate constants of PAPS and DHEA with wild-type and V260E mutant of SULT2A1[a].

SULT2A1	PAPS			DHEA			
	K_m	k_{cat}	k_{cat}/K_m	K_m	k_{cat}	K_i	k_{cat}/K_m
	μM	min^{-1}		μM	min^{-1}	μM	
Wild type	3.9 ± 0.4	8.6 ± 0.8	2.2	4.7 ± 0.3	8.2 ± 0.7	4.3 ± 0.3	1.7
V260E	4.2 ± 0.6	4.4 ± 0.7	1.1	5.6 ± 0.5	4.2 ± 0.5	4.9 ± 0.5	0.8

[a] The reaction mixture with a final volume of 1 ml consisted of 100 mM potassium phosphate buffer at pH 7.0, 5 mM 2-mercaptoethanol, 20 μM PAPS, 2 mM MUS, 5.4 μg K65ER68G of rat SULT1A1, wild type or V260E mutant of SULT2A1 and 5 μM of DHEA at 37 ℃. A linear response was obtained when 14.9 nM (1 μg) SULT2A1 was added in the standard assay condition.

TABLE IV

Dissociation constants of PAP and DHEA in wild-type and V260E mutant of SULT2A1[a].

SULT2A1	Binary complex[b]	Ternary complex[c]
	PAP	DHEA
	nM	*μM*
Wild type	40.7 ± 8.2	0.8 ± 0.05
V260E	36.5 ± 9.7	0.9 ± 0.1

[a] Dissociation constants were determined with spectrofluorimeter as indicated under "Experimental Procedures."

[b] The dissociation constants of binary complex was determined with PAP (5 to 365 nM) and SULT2A1 (100 nM).

[c] The dissociation constants of ternary complex were determined with DHEA (0.1 to 50 μM) and SULT2A1 (0.5 μM) in the presence of PAP (1 μM).

TABLE V

Thermodynamic parameters correlated with free energy of unfolding, $\triangle G_{UN}^{H_2O}$.

SULT2A1	$[Urea]_{50\%}$ [a]	*m* [b]	$\triangle G_{UN}^{H_2O}$ [c]
	M	kcal mol^{-2}	kcal mol^{-1}
Wild type	2.7	2.3 ± 0.3	6.3 ± 0.8
V260E	1.1	1.5 ± 0.2	1.6 ± 0.5

[a] $[Urea]_{50\%}$ is the urea concentration at the midpoint of urea denaturation.

[b] m value is a constant that is proportional to the increase in the degree of exposure of the protein on denaturation.

[c] $\triangle G_{UN}^{H_2O}$ is the free energy of denaturation in the absence of urea, and is the product of $[Urea]_{50\%}$ and *m* value.

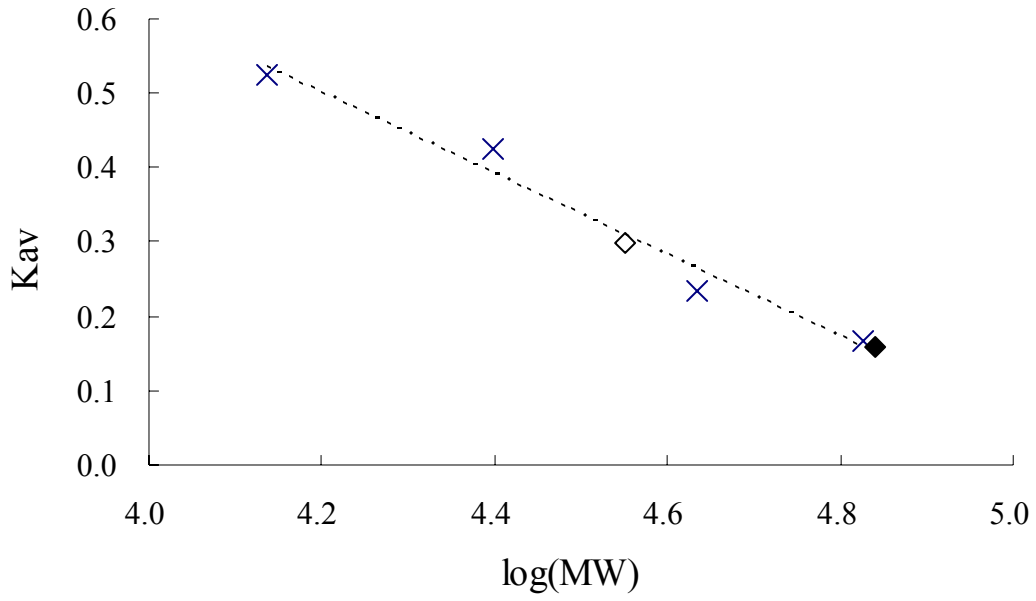

Figure 1. Calibration curve of Sephacryl S-200 HR. A molecular weight calibration curve, which defined the relationship between the elution volumes of a set standards and the logarithm of their respective molecular weights, was determined with Sephacryl S-200 HR. Calibration standards (crisscross) used were ribonuclease A (15.6 KDa), chymotrypsinogen A (19.4 KDa), ovalbumin (47.6 KDa), and Albumin (62.9 KDa). The wild type and V260E mutant were closed and open diamonds, respectively. The Kav is obtained from the equation Kav = (Ve – V0) / (Vt – V0) as described above.

A

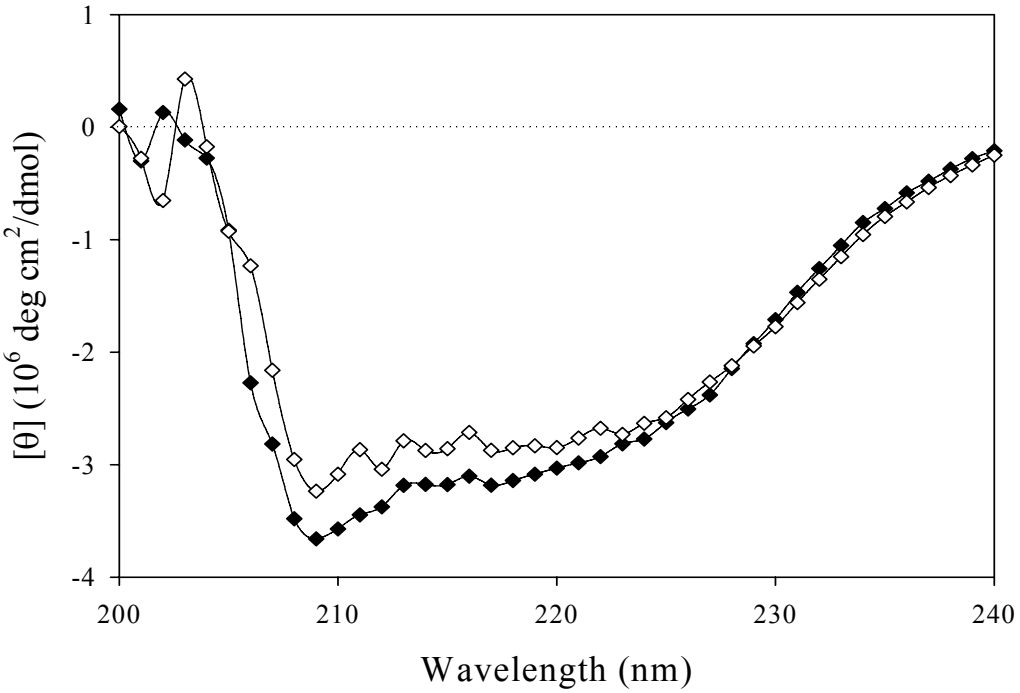
1
0
-1
-2
-3
-4
200
210
220
230
240
[θ] (10^6 deg cm^2/dmol)
Wavelength (nm)

B

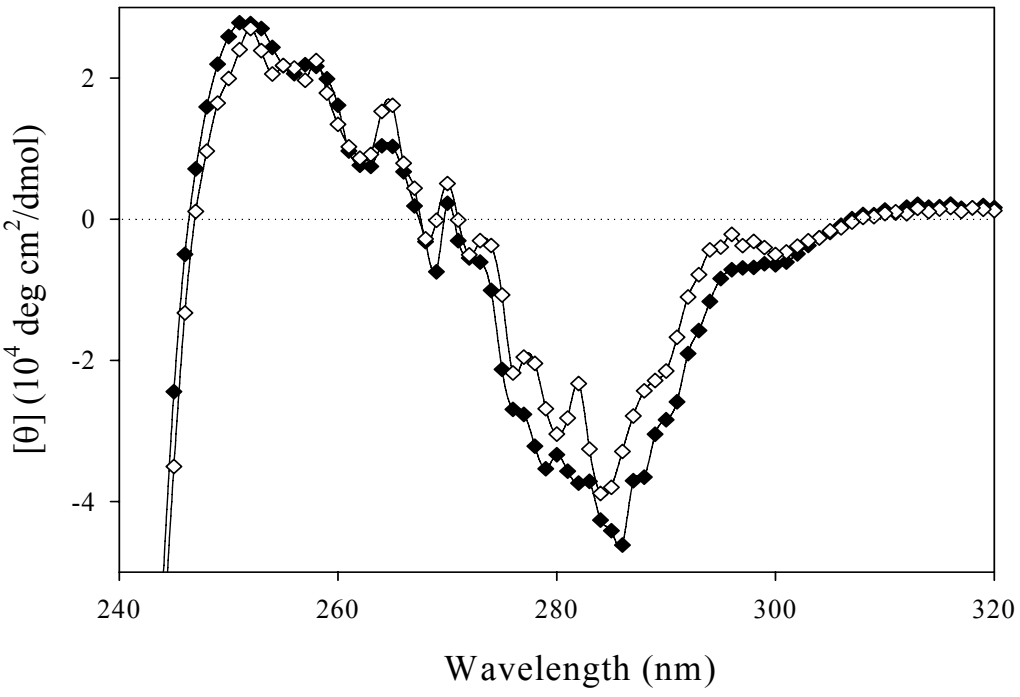
2
0
-2
-4
240
260
280
300
320
[θ] (10^4 deg cm^2/dmol)
Wavelength (nm)

Figure 2. Circular dichroism specrtra of wild-type and V260E mutant of SULT2A1. CD measurements were carried out on a Jasco J715 spectropolarimeter and processed data with J-700 standard analysis version 1.33.00 (Jasco, Japan). CD spectra of enzymes at a concentration of 1 mg ml^{-1} in the phosphate buffer (pH 7.0) were measured in a (*A*) 1 mm light path length quartz cell in the far-UV range (200-240 nm) and (*B*) 1 cm light path in the near-UV (240-320 nm) at room temperature individually. The closed and open diamonds indicated the wild type and V260E mutant of SULT2A1, respectively.

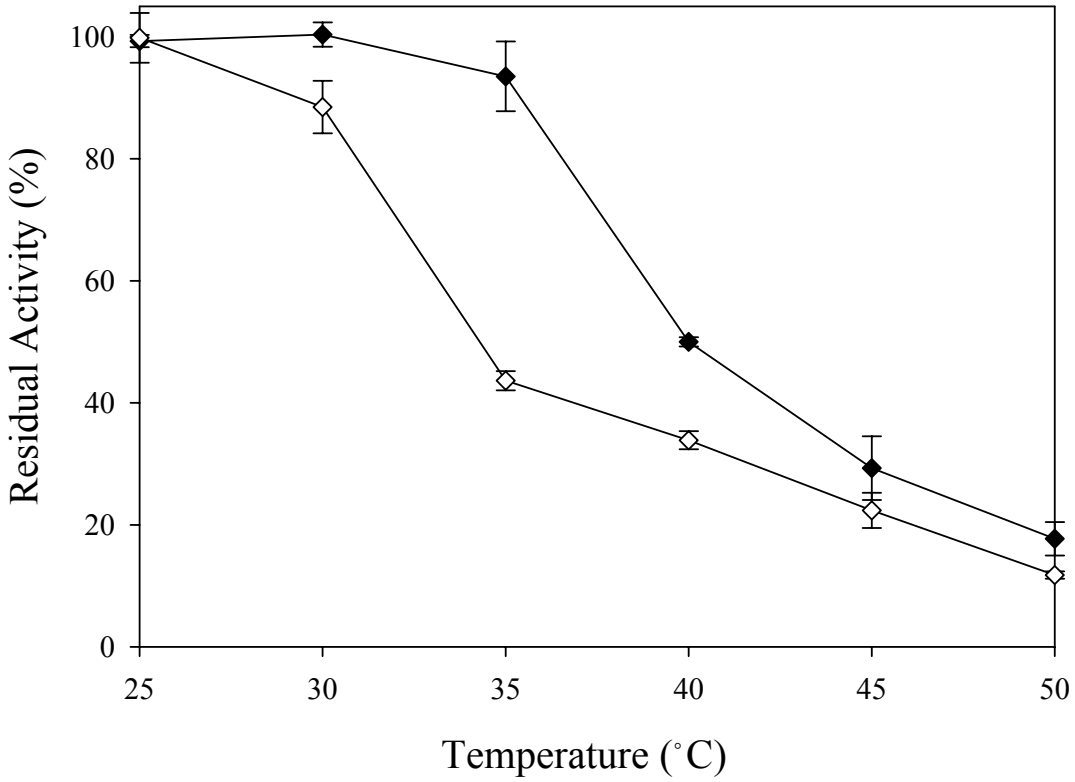

Figure 3. Thermal stability of wild-type and V260E mutant of SULT2A1. Aliquots of wild-type and V260E mutant of SULT2A1 were treated for 15 min at various temperatures and following the enzyme activity assay. The closed and open diamonds indicated the wild type and V260E mutant of SULT2A1, respectively. Each point was determined from duplicate assay data.

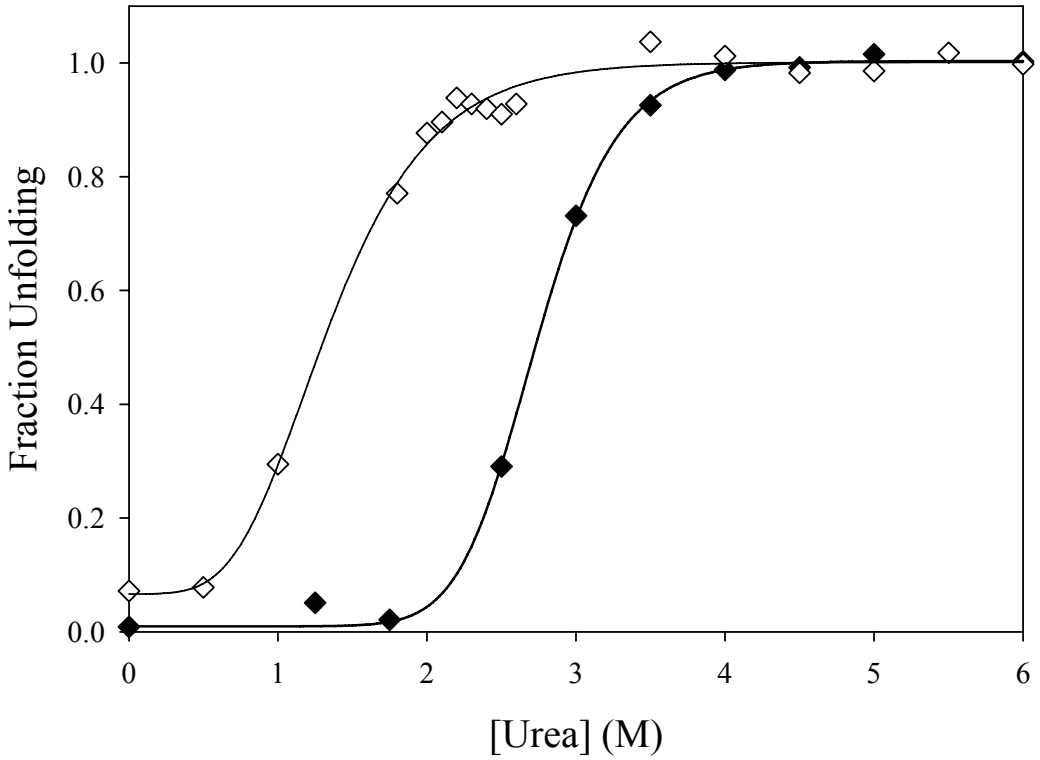

Figure 4. Conformational stability studies. Urea induced equilibrium unfolding monitored by ellipticity at 222 nm on circular dichroism. The unfolding curve for wild-type and V260E mutant were shown by the closed and open diamonds, respectively. These plots show the data normalized (fraction unfolded) taking into accounting the sloping base lines and were obtained using nonlinear regression by SigmaPlot 2001, V7.0 and Enzyme Kinetics Module, V1.1 (SPSS Inc., Chicago, IL).

CHAPTER 3 Met137 and Tyr238 Modulate Substrate Binding Orientation and Inhibition of Human Dehydroepiandrosterone Sulfotransferase

Human dehydroepiandrosterone sulfotransferase (SULT2A1) catalyzes the transfer of the sulfuryl group of 3'-phosphoadenosine 5'-phosphosulfate (PAPS) to hydroxysteroids such as dehydroepiandrosterone (DHEA) and androsterone (ADT). The differences between the complex structures of SULT2A1/DHEA and SULT2A1/PAP or SULT2A1/ADT have enabled us to elucidate the specific amino acids responsible for substrate inhibition. Based on the structural analyses, substitution of the smaller hydrophobic residue alanine for Tyr-238 (Y238A) significantly increases the K_i value for DHEA and totally eliminates substrate inhibition for ADT. In addition, Met-137 was proposed to regulate the binding orientation of DHEA and ADT in SULT2A1.Complete elimination or regeneration of substrate inhibition were demonstrated with the mutations of Met-137 and Tyr-238 in SULT2A1. Analysis of the Met-137 mutants and Met-137/Tyr-238 double mutants uncovered the relationship between substrate binding orientations and inhibition in SULT2A1. Our data indicate that Tyr-238 regulates the release of substrate, and Met-137 controls substrate binding orientation of DHEA and ADT in SULT2A1. In addition, a corresponding residue in other sulfotransferases was shown to have a function similar to that of Tyr-238 in SULT2A1. Experimental results and the multiple structural alignment all indicate that the involvement of this amino acid residue in substrate inhibition may be a general feature in all cytosolic sulfotransferases.

INTRODUCTION

Sulfonation is a widespread biological reaction catalyzed by members of the sulfotransferase (SULT)[1] supergene family. These enzymes catalyze the transfer of a sulfuryl group from 3'-phosphoadenosine 5'-phosphosulfate (PAPS), the universal sulfonate donor molecule, to a substrate acceptor group. Cytosolic sulfotransferases sulfonate small molecules such as drugs, steroid hormones, chemical carcinogens, bile acids, and neurotransmitters (1-6). Some researches (7-17) focus on the critical residues for PAP binding (PSB and PB loop), catalysis (e.g. His-108 in mouse SULT1E1), substrate specificity (Tyr-81 in mouse SULT1E1 and Glu-146 in human SULT1A3), metal ion activation (Asp-86 in human SULT1A3), dimerization motif (KTVE motif near C-terminus), redox effect (Cys-66 and Cys-232 in rat SULT1A1) and substrate inhibition (Phe-247 in human SULT1A1) are shown in **Fig. 1**.

Human dehydroepiandrosterone sulfotransferase (SULT2A1, DHEA-ST) catalyzes the sulfonation of various steroids and their derivatives, including hydroxysteroids such as dehydroepiandrosterone (DHEA), androsterone (ADT), testosterone, estradiol, and many other endogenous steroids (19-22). Steroid sulfonation has been recognized as an important process for maintaining steroid hormone levels during their metabolism. In humans, dehydroepiandrosterone sulfate (DHEAS) is the most prevalent steroid precursor, and is one of the major secretory products of both adult and fetal adrenals (23).

Substrate inhibition is a common characteristic of sulfotransferases (24-29). The catalysis and inhibition of DHEA and ADT by SULT2A1 have been reported to regulate the homeostasis and metabolism of these compounds and to maintain steroid levels (23). Previous studies have suggested that the onset of substrate inhibition is the formation of ternary dead-end complex (30-31). Furthermore, other kinetic studies also indicate that the dead-end complexes of E/PAPS/$ROSO_3$ and E/PAP/ROH can be formed through either sequential

random or ordered Bi Bi kinetic mechanisms (31-35). Recently the substrate inhibition in SULT1A1 has been studied from solved x-ray crystal structure and compared with SULT1A3 which shares 93% amino acid sequence identity (17, 36). The presence of two *p*-nitrophenol (*p*NP) molecules in the crystal structure of SULT1A1 is postulated to explain cooperativity and inhibition at low and high substrate concentrations, respectively. The proposed mechanism of substrate inhibition is that there is impeded catalysis when both binding sites are occupied due to the impeded release of *p*NP[1] that results from molecular crowding. In addition, binding study with human SULT1E1 is shown that the stoichiometry of estradiol binding is two ligands with one enzyme (31). It was proposed that one site is catalytic and that the other is an allosteric site, which regulates turnover. The substrate inhibition in SULT2A1, however, has not been studied in detail yet, even though the solved crystal structure shows the proposed substrate inhibition orientation (37).

Structural alignments among the complex structures of SULT2A1/ADT, SULT2A1/DHEA, and SULT2A1/PAP (23, 37-38) reveal structural variation of amino acids in different substrate and PAP binding states. We herein describe experimental considerations that lead us to propose two of the amino acids, Tyr-238 and Met-137, are residues responsible in regulating substrate inhibition. Finally, we give another experimental example to demonstrate that the corresponding Tyr-238 residues of other cytosolic sulfotransferases possess similar function as that of SULT2A1 and may be a universal feature to regulate substrate inhibition.

EXPERIMENTAL PROCEDURES

Materials—PfuTurbo DNA polymerase was purchased from Stratagene, and MUS, MU, DHEA, ADT, PAP, PAPS, *p*-nitrophenol, dopamine, glutathione (reduced form), and dithiothreitol (DTT) were purchased from Sigma (St. Louis, MO). Potassium phosphate (dibasic) was obtained from J. T. Baker (U.S.A.). DEAE Sepharose fast flow, Glutathione S-transferase Sepharose fast flow and Sephacryl S-100 HR were obtained from Amersham Pharmacia Biotech Asia Pacific (Hong Kong). All other chemicals were obtained commercially at the highest purity possible.

Site-Directed Mutagenesis of the cDNA Encoding SULT2A1, SULT1A1, and SULT1A3—Site-directed mutagenesis was performed with *PfuTurbo* DNA polymerase using QuickChange (Stratagene, La Jolla, CA). All primers for mutagenesis were purchased from Mission Biotech Co., Ltd. (Taiwan). Wild-type SULT2A1, SULT1A1, and SULT1A3 cDNA incorporated in the pGEX-2TK expression vector were used as templates in conjunction with specific mutagenic primers (**Table I**). Mutated cDNA sequences were confirmed using an ABI Prism 377 DNA sequencer (Applied Biosystems, Foster City, CA) following the standard protocol.

Expression, Purification and Characterization of Wild-type and Mutants of SULT2A1, SULT1A1, and SULT1A3—The expression and purification of SULT2A1, SULT1A1, and SULT1A3 were described previously (39-40). Molecular weight of wild type (homodimer) and V260E mutant (monomer) of SULT2A1 was estimated by gel filtration chromatography (15). A homogeneous protein was obtained as determined by SDS-polyacrylamide gel electrophoresis (41).

Enzyme Assay—The activities of wild-type and mutant SULT2A1 were determined according to the change of fluorescence based on a coupled-enzyme assay method (42). The

fluorescence of MU at 460 nm was measured upon excitation at 355 nm. The reaction mixture with a final volume of 1 ml consisted of 100 mM potassium phosphate buffer at pH 7.0, 5 mM 2-mercaptoethanol, 20 μM PAPS, 2 mM MUS, 5.4 μg K65ER68G (43) of rat SULT1A1, SULT2A1 and 5 μM of DHEA or ADT at 37 ℃. A linear response was obtained when 1.49 to 14.9 nM (0.1 to 1 μg) SULT2A1 was added in the standard assay condition (42). In the reaction condition, regeneration of PAPS catalyzed by K65ER68G of rat SULT1A1 is much faster than the production of PAP catalyzed by SULT2A1 for about 40 to 50 folds. SULT1A3 standard assay was similar to the SULT2A1 assay excepts that the reaction mixture contained 1.5 to 7.3 nM (0.1 to 0.5 μg) SULT1A3 and 30 μM of dopamine at 37 ℃. K65ER68G of rat SULT1A1 is inactive toward DHEA, ADT and dopamine in the conditions described above. Activity of SULT1A1 was determined according to the change of absorbency at 400 nm due to elimination of free *p*-nitrophenol (ε = 10500 $M^{-1}cm^{-1}$ at pH 7.0) as described previously (43). The reaction mixture consisted of 100 mM potassium phosphate buffer at pH 7.0, 1 to 100 nM (0.07 to 7 μg) SULT1A1, 50 μM PAPS, 5 mM 2-mercaptoethanol, and 5 μM *p*-nitrophenol at 37 ℃.

Substrate Binding—The dissociation constants (K_d) of PAP, DHEA, ADT towards SULT2A1, respectively, were determined with a spectrofluorimeter as described previously (31). The decrease in intrinsic fluorescence of protein at 340 nm was observed upon excitation at 280 nm when an aliquot amount of PAP was added into the mixture consisted of 100 mM potassium phosphate buffer at pH 7.0, 100 nM wild-type or mutant SULT2A1 and varying concentrations of PAP at 25 ℃ with a final volume of 1.3 ml in a quartz cuvette of 1 cm square cross-section. In the formation of ternary dead-end complex, DHEA and ADT were added into the pre-incubated solution containing 0.5 μM wild type or mutants of SULT2A1, 100 mM potassium phosphate at pH 7.0, and 1 μM PAP at 25 °C. Each data point was

duplicated, and the difference was within 10%.

Molecular Modeling—Homology modeling of the M137I and M137W mutants were constructed using the SWISS-MODEL server (44) based on the SULT2A1/DHEA complex structure (PDB code: 1J99) (37). These modeled structures were used in GOLD (45) as templates to dock DHEA and ADT molecules with 10 genetic algorithm runs. Figures were prepared using Swiss-Pdb Viewer (46).

Analysis of Kinetic Data—Results of kinetic experiments were analyzed using nonlinear regression to fit the appropriate equation to the data. Kinetic data obtained from non-inhibitory experiments were individually fit to Michaelis-Menten Equation 1, and substrate inhibition data were fitted to substrate inhibition in Equation 2 (47). The rate constants (K_m, V_{max}, and K_i) were obtained using SigmaPlot 2001, V7.0 and Enzyme Kinetics Module, V1.1 (SPSS Inc., Chicago, IL). Data used represent mean values derived from two determinations.

$$v = V[S]/(K_m + [S]) \quad \text{(Eq. 1)}$$

$$v = V[S]/\{K_m + [S](1 + [S]/K_i)\} \quad \text{(Eq. 2)}$$

Crystallization and Data Collection—M137I and M137W mutants of SULT2A1 were co-crystallized with DHEA and ADT using the hanging drop vapor diffusion technique at room temperature (48). Proteins were concentrated at 10 mg/ml and either 0.5 mM DHEA or ADT in 10 mM Tris, pH 7.5, and 0.1% n-octyl β-D-glucopyranoside (β-OG). Drops were prepared by mixing equal volumes of protein and reservoir solutions consisting of 100 mM HEPES, pH 7.5, 100 mM sodium chloride, and 1.6 M ammonium sulfate. The crystals appeared after 2–3 days and matured in 7–10 days.

RESULTS

Predicting Critical Amino Acid Residue for Substrate Inhibition by the Comparison of the Structure of SULT2A1 Complexes—Crystal structures of SULT2A1 containing ADT, DHEA, and PAP, respectively, have been reported (23, 37-38). It has been proposed that substrate inhibition was induced due to the formation of the enzyme/PAP/substrate ternary complex (30-31). Comparison between the SULT2A1/PAP and SULT2A1/DHEA binary complex structures may reveal the alternative locations of the main regulatory amino acid residues when substrate is present or absent in the active site. The overall structure of the SULT2A1/PAP complex is very similar to that of the SULT2A1/DHEA complex, except for some residues and a loop from residues Tyr-231 to Gly-252 (**Table II**). The root-mean-square deviation (RMSD) value of this loop between the two structures is 6.67 Å for the backbone (excluding Lys-242 and Thr-243, which were not solved in the SULT2A1/PAP binary complex structure). As shown in **Fig. 2*A***, the main difference in the DHEA binding site between the two complexes is that the loop from residues Tyr-231 to Tyr-238 is closed in SULT2A1/PAP, while it is open in SULT2A1/DHEA (37-38). Furthermore, in the SULT2A1/DHEA complex, several hydrophobic residues on this loop, including Tyr-231, Leu-234, and Tyr-238, are located in close proximity to the DHEA molecule; these residues contribute to the hydrophobic nature of the active site. Also, in the SULT2A1/DHEA binary complex structure, Tyr-238 acts likely as the gate toward the substrate-binding cavity, but moves away from the active site in the SULT2A1/PAP binary complex structure (**Fig. 2*A***). It is therefore reasonable to speculate that Tyr-238 may play a critical role in regulating the release of substrate. Two distinct DHEA orientations have been revealed in the SULT2A1/DHEA complex structure (37). By contrast, ADT exhibited only one substrate orientation in the active site of the SULT2A1/ADT complex (23). As shown in **Fig. 2*B***, the

ADT molecule shares the same location as that of the DHEA molecule in the previously proposed alternative orientation (37). The SULT2A1/DHEA and SULT2A1/ADT complex structures are quite similar at this region, including the loop described above, and the location of Tyr-238 residue. The origin and biological significance of the two proposed orientations of DHEA have not been studied well so far. The structural comparison described above reveals that the previously proposed catalytic orientation for DHEA (37) disagrees with that for ADT. Mutational studies and kinetic evidences will be provided later to show that ADT which contains only one substrate orientation in SULT2A1 should be in the catalytic orientation.

Kinetic Analysis of Tyr-238 Mutants of SULT2A1—The hypothesized gate residue of Tyr-238 for regulating substrate inhibition, as revealed by the above structural comparison, was confirmed by site-directed mutagenesis. V_{max}, K_m and K_i values of wild type and Tyr-238 mutants (Y238A, Y238F, and Y238W of SULT2A1) were determined using DHEA or ADT as substrates (**Table III**). Y238A of SULT2A1 exhibited no substrate inhibition when ADT was used as substrate and the K_i value of DHEA was significantly increased. The K_i values of DHEA and ADT for Y238F and Y238W of SULT2A1 were either only slightly higher than those of wild type or within the error tolerance, respectively. The changes of K_m and V_{max} for Y238A, Y238F and Y238W were not drastic whenever DHEA or ADT was used as substrate (**Table III**). This observation, consistent with the above prediction base on structural analysis, showed that Y238 is regulating the substrate inhibition and demonstrated that the size of the amino acid side chain (Y238) is important.

Predicting Amino Acid Residue Delineates the Orientations of DHEA and ADT in SULT2A1—Mutating Tyr-238 to alanine completely and partially eliminate substrate inhibition for ADT and DHEA, respectively (**Table III**), indicating that additional amino acid(s) may be interacting with these two substrates in a different way. The complex structures of SULT2A1/DHEA and SULT2A1/ADT revealed two orientations for DHEA but

only one for ADT as described earlier (23). From the available information, we might infer that the additional amino acid(s) that affect substrate inhibition of DHEA may also affect its binding orientation in SULT2A1. To search for the possible amino acid(s), we superimposed the structures of SULT2A1/DHEA and SULT2A1/ADT on each other. Most of the amino acid residues hold the same positions in the two complex structures, except for the side chains of Met-16, Ile-71, and Met-137 whose RMSD values (2.41, 2.50, and 2.40 Å, respectively) (**TABLE IV**) are noticeably higher than those of the others (**Fig. 3**). Both Met-16 and Ile-71 of the SULT2A1/DHEA and SULT2A1/ADT complex structures form similar van der Waals interactions toward ADT and DHEA in the two orientations. By contrast, the C_ε atom of the Met-137 residue in SULT2A1/ADT complex structure points inward the substrate binding site and causes steric hindrance for ADT and prevents it from forming additional orientation observed only for DHEA. The shortest distance would have been only 1.11 Å between C-12 of DHEA at this additional orientation and the C_ε atom of Met-137 in SULT2A1/ADT complex (**Fig. 3**). From the structural analysis between SULT2A1/DHEA and SULT2A1/ADT complexes, it is reasonable to propose that, in addition to Tyr-238, Met 137 may serve as the amino acid that modulates the substrate inhibition and binding orientations of DHEA and ADT.

Kinetic Analysis of Met-137 and Met-137/Tyr-238 Mutants of SULT2A1—The proposed effects of Met-137 on substrate inhibition were examined by mutational analysis of SULT2A1 at Met-137 and Tyr-238. Significantly larger K_i values (over one order of magnitude) for ADT were obtained (**Table III**) when Met-137 of SULT2A1 was mutated to isoleucine (M137I) and valine (M137V) which contain smaller side chains. Such effect was less significant when Met-137 of SULT2A1 was mutated to amino acid with larger side chain, tryptophane (M137W). Changes of K_i values for DHEA were less significant as compared to those for ADT (**Table III**). M137K was also prepared and exhibited no enzymatic activity, most

probably due to the positive charge of lysine that interferes with the hydrophobicity of the binding site. These observations are consistent with the above structural analysis that Met-137 side chain is a steric hindrance for ADT in SULT2A1/ADT complex but not for DHEA in SULT2A1/DHEA complex (**Fig. 3**). By removing this steric hindrance, additional binding orientation for ADT may form and may cause substrate inhibition that can not be removed by mutating Tyr-238 as described above (**Table III**). In contrast, by adding a large side chain at Met-137, the additional binding orientation of DHEA may be removed and the substrate inhibition may be completely eliminated with Tyr-238 mutant. Double mutations at Met-137 and Tyr-238 confirm our hypothesis. Mutation of SUKT2A1 Y238A mutant (which exhibit no ADT substrate inhibition as shown in **Table III**) at Met-137 produces a double mutant, M137I/Y238A, which exhibits ADT substrate inhibition (**Table III**). Similarly, mutation of Y238A (this mutation can not completely remove DHEA substrate inhibition) at Met-137 produces a double mutant, M137W/Y238A, which exhibits no DHEA substrate inhibition (**Table III**). The large side chain of tryptophane may prevent DHEA from forming the additional orientation in M137W/Y238A so that no substrate inhibition can be observed. Two other double mutants, M137V/Y238A and M137K/Y238A (**Table III**), also exhibited expected properties. The K_i values obtained with M137V/Y238A were between those obtained with M137I/Y238A and M137W/Y238A. M137K/Y238A still exhibited no enzymatic activity as that of M137K.

Molecular Modeling of DHEA and ADT binding orientations in SULT2A1—The data discussed above also indicate that the additional substrate orientation modulated by Met-137 is not a catalytic active orientation and the presence of this binding orientation is to generate additional substrate inhibition. The orientations of DHEA and ADT in M137I and M137W were modeled by SWISS-MODEL and GOLD (44-45) as shown in **Fig. 4**. Two substrate orientations and one substrate orientation were obtained for M137I and M137W, respectively.

These modeled structures are consistent with the substrate inhibition data discussed and shown in **Table III** that Met-137 modulate the substrate binding orientations and can be demonstrated by site-directed mutagenesis. As shown in **Fig. 4*A***, the sulfonation sites of DHEA or ADT are facing in two different orientations. It is reasonable to speculate that only one of the orientations is catalytically active and should be the one as shown in **Fig. 4*B***. As shown in **Table III**, substrate inhibition was completely eliminated when substrate existed only one substrate orientation but not in two orientations in Y238A mutant. It is also reasonable to speculate that the additional orientation existed is responsible for the substrate inhibition observed.

Substrate Inhibition of SULT2A1 Monomer—In a previous study on SULT2A1/PAP complex structure (38), the loop (residues 231-252, shown in **Fig. 2*A***) was speculated to prevent substrate binding while being involved in the dimer interface. This implies that the dimer may be an inactive form, with the second subunit of the dimer contributing to the locking in the substrate-blocking loop. To examine the previous hypothesis that dimerization results in substrate blocking, the monomer mutant (V260E) of SULT2A1, designated in the KTVE motif (15) along with a double mutant, Y238A/V260E (**Table III**), were constructed to comprehend the substrate inhibition of SULT2A1. The wild-type SULT2A1 (homodimer) was found to have similar kinetic constants as those of the mutant monomer. Furthermore, the pattern of substrate inhibition in monomer mutant (V260E in **Table III**) is the same as that of wild-type SULT2A1. The mutation of mutant monomer at Tyr-238 (Y238A/V260E in **Table III**) also gives exactly the same substrate inhibition pattern as that of Y238A of SULT2A1 (**Table III**). Data obtained from this study indicates that dimer or monomer of SULT2A1 does not play an important role for the exhibition of substrate inhibition.

Dissociation Constants of PAP, DHEA and ADT in Binary and Ternary Dead-end Complex of SULT2A1 and Its Mutants—The cause of sulfotransferae substrate inhibition has

been attributed to the formation of an enzyme, substrate and PAP ternary complex (30-31). The binding of PAP is critical for the formation of the ternary complex (9) and it has been shown that affinity of PAP had profound effects on the activity of sulfotransferases (35, 43). It is important to show that this ternary complex is intact in SULT2A1 mutants: Y238A, M137I, M137W, M137I/Y238A and M137W/Y238A to support our proposal that M137 and Y238 directly modulate substrate inhibition. Circular dichroism spectra of SULT2A1 and its mutants were obtain to demonstrate that their secondary structures remain intact (**Fig. 5**). As shown in **Table V**, the dissociation constants of PAP for the formation of the SULT2A1/PAP binary complexes remain the same among wild type and all the mutants. Tight binding of PAP (in nM range as shown in **Table V**) to the SULT2A1 and its mutants indicates that PAP binding site remains intact following such mutations. This information excludes the possibility that the change of K_i values reported in this study is due to the change of PAP binding to SULT2A1 mutants.

Affinity of either DHEA or ADT to SULT2A1/PAP binary complex was significantly decreased with Y238A mutant as compared to that of wild type enzyme (**Table V**). In contrast, mutation at Met-137 (M137I or M137W) did not significantly affect the bonding of either DHEA or ADT to the enzyme binary complex. The dissociation constants of the double mutants of SULT2A1, M137I/Y238A and M137W/Y238A, are very similar to those of single mutant, Y238A (**Table V**). These observations are consistent with the proposed function of Tyr-238 and Met-137 that the former acts to prevent the release of bound substrates while the later modulates the orientation of bound substrates.

Functional Analysis of Tyr-238 Corresponding Residues in Other Sulfotransferases—The multiple sequence and structure alignments of some solved-structure sulfotransferases are shown in **Fig. 6**. The residues corresponding to Tyr-238 of SULT2A1 have been highlighted, and they are as follows: Phe-247 of human SULT1A1, Leu-247 of human SULT1A3, Met-247

of mouse SULT1E1, Leu-249 of human SULT2B1_v1 (36, 50-52). This comparison leads us to hypothesize that the Tyr-238 corresponding residue in other sulfotransferases may play a similar role in substrate inhibition because these residues all demonstrate steric hindrance of the substrate-binding cavity, and therefore they may modulate substrate inhibition for their own preferred substrates. To characterize the corresponding residues of Tyr-238 of SULT2A1 in other sulfotransferases, further mutational analysis was conducted with SULT1A1 and SULT1A3 at Phe-247 and Leu-247 residue, respectively (**Table VI**). As compared to those of wild type SULT1A1, the K_i value of F247A (with *p*-nitrophenol as substrate) increased approximately 12-fold, while the V_{max}/K_m value increased approximately 3-fold. The K_i value of dopamine for SULT1A3 is much higher than that of *p*NP for SULT1A1 (**Table VI**). It may presumably due to the positive charged dopamine at the assay condition. Mutations at Leu-247 of SULT1A3 give K_i values comparable with the size of the side chain of the mutated amino acid as shown in **Table VI** for L247A and L247Y (the larger the amino acid side chain, the lower the K_i value). The data from these investigations support our hypotheses that substrate inhibition in SULT2A1 is modulated by Tyr-238, and that analogous residues of Tyr-238 in other sulfotransferases play similar roles with respect to substrate inhibition.

DISCUSSION

Recently, there has been an increase in structure/function studies as a result of an expansion of solved x-ray crystal structures of sulfotransferases. DHEA has been proposed to have two binding orientations in SULT2A1 (37), however, bound ADT possesses only one, in which it is flipped over along the long axis of the DHEA relative to the proposed alternative orientation (23). The proposed alternative orientation of DHEA was speculated to be a substrate-inhibition orientation owing to the fact that it placed O-3 hydroxyl group of DHEA with respect to His-99 for 2.9 Å away, and closer to the modeled PAP. Furthermore, it contained more van der Waals interactions with hydrophobic residues than the catalytic orientation (37). Gamage *et al.* (53), however, suggested that this would not result in substrate inhibition because this would require a relative increase in the proportion of the proposed alternative orientation while the substrate concentration increases. It might infer that both the orientations of DHEA could cause substrate inhibition while PAP remained in the active site to form ternary dead-end complex. In this report, we identified two amino acids (Met-137 and Tyr-238) responsible for modulating substrate inhibition of DHEA and ADT and were able to provide experimental evidences to show that both substrate binding orientations of SULT2A1 indeed cause substrate inhibition.

The bound orientations observed for DHEA and ADT might be the substrate inhibition mode because the crystals were usually formed under high concentration of ligands although PAP was not present in the solved crystal structures of SULT2A1/DHEA and SULT2A1/ADT (23, 37). K_i values of DHEA for SULT2A1 and its mutants at Tyr-238 and Met-137 (**Table III**) also support that substrate inhibition may be induced by two possible binding modes for DHEA. According to the crystal structures of SULT2A1 (**Fig. 2**), Tyr-238 has weak interactions with ADT and the two orientations of DHEA as the closest distance is

about 4.6 Å. It strongly suggests that Tyr-238 acts as a gate residue to regulate the release of substrate into the substrate-binding cavity. The dissociation constants of ternary dead-end complex shown in **Table V** also support this implication. K_d of both DHEA and ADT increase significantly when Tyr-238 was mutated to alanine. However, mutation of Tyr-238 alone can not completely eliminate DHEA substrate inhibition (**Table III**) indicating the existence of an additional substrate inhibition mode for DHEA but not for ADT. Structural analysis showed that Met-137 is closely interacting with DHEA and ADT and may modulate the substrate binding orientation (**Fig. 3**). This observation agrees with the experimental data that further mutation of Y238A at Met-137 not only can completely eliminate substrate inhibition for DHEA (M137W/Y238A in **Table III**) but can also create substrate inhibition for ADT (M137I/Y238A in **Table III**). These data strongly suggest that, in these double mutants, DHEA exists in only one orientation (M137W/Y238A) and ADT presents in two orientations (M137I/Y238A). Molecular calculation and modeling shown in **Fig. 4** give additional support for the proposed substrate binding orientations in these mutants.

Other possible causes for substrate inhibition proposed previously were also examined in this study (15). Dimerizatin of SULT2A1 is shown to have nothing to do with the substrate inhibition for exactly the same substrate inhibition patterns were observed for enzyme monomer, dimer and their mutants (**Table III**). Binding of PAP may significantly affect the substrate binding (9) and in turn affect substrate inhibition. This possibility was also examined to show that mutation at Met-137 and Tyr-238 did not affect the nucleotide binding affinity with SULT2A1 (**Table V**). In addition, the increase of the dissociation constants of DHEA and ADT in Tyr-238 and Met-137 mutants (**Table V**) is consistent with what would be expected for the partial or complete elimination of substrate inhibition.

The overall model of the modulation by Met-137 and Tyr-238 for substrate binding orientation and inhibition is shown in **Fig. 7**. The wild type SULT2A1 exhibits substrate

inhibition for DHEA and ADT while the PAP is present simultaneously. In the mutant Y238A, there is no substrate inhibition for ADT and less significant substrate inhibition for DHEA. Mutation at Met-137 proposed to regulate the substrate binding orientation in this study, uncover the relationship between the substrate binding orientations and substrate inhibition while Y238A is examined. Mutation at Met-137 alone does not significantly change the substrate inhibition pattern for both DHEA and ADT. For Y238A mutant, however, the size of Met-137 side chain can modulate the substrate inhibition pattern for DHEA and ADT. Thus the double mutant at Met-137 and Tyr-238 can significantly convert the substrate inhibition pattern of Y238A. In **Fig. 6**, two substrate binding orientations are shown and they are proposed to have different substrate inhibition patterns.

Finally, the function of Tyr-238 corresponding position in SULT2A1 is proposed to be a general feature among other cytosolic sulfotrasnferases. Previous researches on substrate inhibition of SULT1A1 (17, 36) revealed that SULT1A1 could accommodate two *p*-nitrophenol which leads to the substrate inhibition. In our study the Phe-247 of SULT1A1, which corresponds to Tyr-238 of SULT2A1, confirm that substrate inhibition can be similarly regulated and they all play the role to prevent the substrate from releasing. (**Table VI**). Furthermore, the corresponding residue in SULT1A3, leucine, is mutated to alanine and a higher K_i value is obtained for dopamine (**Table VI**). Replacing this leucine with tyrosine and phenylalanine decrease the K_i values (**Table VI**). We therefore propose that the Tyr-238 and its corresponding residues in other cytosolic sulfotransferases play the similar role on regulating the release of substrate.

To further confirm the hypothesis that Met-137 could modulate substrate binding orientations and then regulate the substrate inhibition, the cocrystalization of DHEA and ADT with M137I and M137W are performed. So far homogeneous enzymes (M137I and M137W) are purified (**Fig. 8**) and the co-crystals of individual enzymes and substrate are produced (**Fig.**

9) The phase determination is still in progress.

In conclusion, we propose that the substrate inhibition in sulfotransferase could occur either from the formation of ternary dead-end complex or the mis-orientation of substrate in the complex (53). The proposed function of Tyr-238 and Met-137 in SULT2A1 in this study may also be a model to explain how the substrate inhibition is modulated in other sulfotransferases.

REFERENCES

1. Mulder, G. J., and Jakoby, W. B. (1990) in *Conjugation Reactions in Drug Metabolism* (Mulder, G. J., ed) pp. 107–161, Taylor and Francis, Ltd., London
2. Falany, C., and Roth, J. A. (1993) in *Human Drug Metabolism: From Molecular Biology to Man* (Jeffery, E. H., ed) pp. 101–115, CRC Press, Inc. Boca Raton, FL
3. Weinshilboum, R., and Otterness, D. (1994) in *Conjugation-Deconjugation Reactions in Drug Metabolism and Toxicity* (Kaufmann, F. C., ed) pp. 45–78, Springer-Verlag, Berlin
4. DeBaun, J. R., Miller, E. C., and Miller, J. A. (1970) N-hydroxy-2-acetylaminofluorene sulfotransferase: its probable role in carcinogenesis and in protein-(methion-S-yl) binding in rat liver. *Cancer Res.* **30,** 577–595
5. Glatt, H. (1997) Sulfation and sulfotransferases 4: bioactivation of mutagens via sulfation. *FASEB J.* **11,** 314–321
6. Falany, C. N. (1997) Sulfation and sulfotransferases. Introduction: changing view of sulfation and the cytosolic sulfotransferases. *FASEB J.* **11,** 1–2
7. Kakuta, Y., Pedersen, L. G., Pedersen, L. C., and Negishi, M. (1998) Conserved structural motifs in the sulfotransferase family. *Trends Biochem. Sci.* **23,** 129–130
8. Kakuta, Y., Petrotchenko, E. V., Pedersen, L. C., and Negishi, M. (1998) The sulfuryl transfer mechanism. Crystal structure of a vanadate complex of estrogen sulfotransferase and mutational analysis. *J. Biol. Chem.* **273,** 27325–27330
9. Hsiao, Y. S., and Yang, Y. S. (2002) A single mutation converts the nucleotide specificity of phenol sulfotransferase from PAP to AMP. *Biochemistry* **41**, 12959–12966
10. Marsolais, F., and Varin, L. (1997) Mutational analysis of domain II of flavonol 3-sulfotransferase. *Eur. J. Biochem.* **247,** 1056–1062
11. Petrotchenko, E. V., Doerflein, M. E., Kakuta, Y., Pedersen, L. C., and Negishi, M. (1999)

Substrate gating confers steroid specificity to estrogen sulfotransferase. *J. Biol. Chem.* **274,** 30019–30022

12. Dajani, R., Hood, A. M., and Coughtrie, M. W. (1998) A single amino acid, glu146, governs the substrate specificity of a human dopamine sulfotransferase, SULT1A3. *Mol. Pharmacol.* **54,** 942–948
13. Pai, T. G., Ohkimoto, K., Sakakibara, Y., Suiko, M., Sugahara, T., and Liu, M. C. (2002) Manganese stimulation and stereospecificity of the Dopa (3,4-dihydroxyphenylalanine)/tyrosine-sulfating activity of human monoamine-form phenol sulfotransferase. Kinetic studies of the mechanism using wild-type and mutant enzymes. *J. Biol. Chem.* **277**, 43813–43820
14. Pai, T. G., Oxendine, I., Sugahara, T., Suiko, M., Sakakibara, Y., and Liu, M. C. (2003) Structure-function relationships in the stereospecific and manganese-dependent 3,4-dihydroxyphenylalanine/tyrosine-sulfating activity of human monoamine-form phenol sulfotransferase, SULT1A3. *J. Biol. Chem.* **278,** 1525–1532
15. Petrotchenko, E. V., Pedersen, L. C., Borchers, C. H., Tomer, K. B., and Negishi, M. (2001) The dimerization motif of cytosolic sulfotransferases. *FEBS Lett.* **490,** 39–43
16. Marshall, A. D., Darbyshire, J. F., Hunter, A. P., McPhie, P., and Jakoby, W. B. (1997) Control of activity through oxidative modification at the conserved residue Cys66 of aryl sulfotransferase IV. *J. Biol. Chem.* **272,** 9153–9160
17. Barnett, A. C., Tsvetanov, S., Gamage, N., Martin, J. L., Duggleby, R. G., and McManus, M. E. (2004) Active site mutations and substrate inhibition in human sulfotransferase 1A1 and 1A3. *J. Biol. Chem.* **279,** 18799–18805
18. Thompson, J. D., Higgins, D. G., and Gibson, T. J. (1994) CLUSTAL W: improving the sensitivity of progressive multiple sequence alignment through sequence weighting, position-specific gap penalties and weight matrix choice. *Nucleic Acids Res*. **22,**

4673–4680

19. Falany, C. N. (1997) Enzymology of human cytosolic sulfotransferases. *FASEB J.* **11,** 206–216

20. Weinshilboum, R. M., Otterness, D. M., Aksoy, I. A., Wood, T. C., Her, C., and Raftogianis, R. B. (1997) Sulfation and sulfotransferases 1: Sulfotransferase molecular biology: cDNAs and genes. *FASEB J.* **11,** 3–14

21. Chen, G., Banoglu, E., and Duffel, M. W. (1996) Influence of substrate structure on the catalytic efficiency of hydroxysteroid sulfotransferase STa in the sulfation of alcohols. *Chem. Res. Toxicol.* **9,** 67–74

22. Kakuta, Y., Pedersen, L. C., Chae, K., Song, W. C., Leblanc, D., London, R., Carter, C. W., and Negishi, M. (1998) Mouse steroid sulfotransferases: substrate specificity and preliminary X-ray crystallographic analysis. *Biochem. Pharmacol.* **55,** 313–317

23. Chang, H. J., Shi, R., Rehse, P., and Lin, S. X. (2004) Identifying androsterone (ADT) as a cognate substrate for human dehydroepiandrosterone sulfotransferase (DHEA-ST) important for steroid homeostasis: structure of the enzyme-ADT complex. *J. Biol. Chem.* **279,** 2689–2696

24. Otterness, D. M., Wieben, E. D., Wood, T. C., Watson, W. G., Madden, B. J., McCormick, D. J., and Weinshiboum, R. M. (1992) Human liver dehydroepiandrosterone sulfotransferase: molecular cloning and expression of cDNA. *Mol. Pharmacol.* **41,** 865–872

25. Sugiyama, Y., Stolz, A., Sugimoto, M., Kuhlenkamp, J., Yamada, T., and Kaplowitz, N. (1984) Identification and partial purification of a unique phenolic steroid sulphotransferase in rat liver cytosol. *Biochem. J.* **224,** 947–953

26. Marcus, C. J., Sekura, R. D., and Jakoby, W. B. (1980) A hydroxysteroid sulfotransferase from rat liver. *Anal. Biochem.* **107,** 296–304

27. Raftogianis, R. B., Wood, T. C., and Weinshilboum, R. M. (1999) Human phenol sulfotransferases SULT1A2 and SULT1A1: genetic polymorphisms, allozyme properties, and human liver genotype-phenotype correlations. *Biochem. Pharmacol.* **58,** 605–616

28. Reiter, C., Mwaluko, G., Dunnette, J., Van Loon, J., and Weinshilboum, R. (1983) Thermolabile and thermostable human platelet phenol sulfotransferase. Substrate specificity and physical separation. *Naunyn Schmiedebergs Arch. Pharmacol.* **324,** 140–147

29. Ganguly, T. C., Krasnykh, V., and Falany, C. N. (1995) Bacterial expression and kinetic characterization of the human monoamine-sulfating form of phenol sulfotransferase. *Drug Metab. Dispos.* **23,** 945–950

30. Duffel, M. W., and Jakoby, W. B. (1981) On the mechanism of aryl sulfotransferase. *J. Biol. Chem.* **256,** 11123–11127

31. Zhang, H., Varlamova, O., Vargas, F. M., Falany, C. N., and Leyh, T. S. (1998) Sulfuryl transfer: the catalytic mechanism of human estrogen sulfotransferase. *J. Biol. Chem.* **273,** 10888–10892

32. Varin, L., and Ibrahim, R. K. (1992) Novel flavonol 3-sulfotransferase. Purification, kinetic properties, and partial amino acid sequence. *J. Biol. Chem.* **267,** 1858–1863

33. Banerjee, R. K., and Roy, A. B. (1968) Kinetic studies of the phenol sulphotranferase reaction. *Biochim. Biophys. Acta.* **1513,** 573–586

34. Pennings, E. J., Vrielink, R., and van Kempen, G. M. (1978) Kinetics and mechanism of the rat brain phenol sulphotransferase reaction. *Biochem. J.* **173,** 299–307

35. Marshall, A. D., McPhie, P., and Jakoby, W. B. (2000) Redox control of aryl sulfotransferase specificity. *Arch. Biochem. Biophys.* **382,** 95–104

36. Gamage, N. U., Duggleby, R. G., Barnett, A. C., Tresillian, M., Latham, C. F., Liyou, N. E., McManus, M. E., and Martin, J. L. (2003) Structure of a human carcinogen-converting

enzyme, SULT1A1. Structural and kinetic implications of substrate inhibition. *J. Biol. Chem.* **278,** 7655–7662

37. Rehse, P. H., Zhou, M., and Lin, S. X. (2002) Crystal structure of human dehydroepiandrosterone sulphotransferase in complex with substrate. *Biochem. J.* **364,** 165–171
38. Pedersen, L. C., Petrotchenko, E. V., and Negishi, M. (2000) Crystal structure of SULT2A3, human hydroxysteroid sulfotransferase. *FEBS Lett.* **475,** 61–64
39. Chang, H. J., Zhou, M., and Lin, S. X. (2001) Human dehydroepiandrosterone sulfotransferase: purification and characterization of a recombinant protein. *J. Steroid Biochem. Mol. Biol.* **77,** 159–165
40. Sakakibara, Y., Takami, Y., Nakayama, T., Suiko, M., and Liu, M. C. (1998) Localization and functional analysis of the substrate specificity/catalytic domains of human M-form and P-form phenol sulfotransferases. *J. Biol. Chem.* **273,** 6242–6247
41. Laemmli, U. K. (1970) Cleavage of structural proteins during the assembly of the head of bacteriophage T4. *Nature* **227,** 680–685
42. Chen, W. T., Liu, M. C., and Yang, Y. S. (2005) Fluorometric assay for alcohol sulfotransferase. *Anal. Biochem.* **339,** 54–60
43. Yang, Y. S., Marshall, A. D., McPhie, P., Guo, W. X., Xie, X., Chen, X., and Jakoby, W. B. (1996) Two phenol sulfotransferase species from one cDNA: nature of the differences. *Protein Expr. Purif.* **8,** 423–429
44. Schwede, T., Kopp, J., Guex, N., and Peitsch, M. C. (2003) SWISS-MODEL: An automated protein homology-modeling server. *Nucleic Acids Res.* **31,** 3381–3385
45. Jones, G., Willett, P., Glen, R. C., Leach, A. R., and Taylor, R. (1997) Development and validation of a genetic algorithm for flexible docking. *J. Mol. Biol*. **267**, 727–748
46. Guex, N., and Peitsch, M. C. (1997) SWISS-MODEL and the Swiss-PdbViewer: an

environment for comparative protein modeling. *Electrophoresis* **18,** 2714–2723

47. Cornish-Bowden, A. (1995) *Analysis of Enzyme Kinetic Data*, pp. 118–122, Oxford University Press, Oxford
48. McPherson, A. (1999). *Crystallization of Biological Macromolecules*, pp. 188, Cold Spring Harbor Laboratory Press.
49. Shindyalov, I. N., and Bourne, P. E. (1998) Protein structure alignment by incremental combinatorial extension (CE) of the optimal path. *Protein Eng.* **11,** 739–747
50. Lu, J. H., Li, H. T., Liu, M. C., Zhang, J. P., Li, M., An, X. M., and Chang, W. R. (2005) Crystal structure of human sulfotransferase SULT1A3 in complex with dopamine and 3'-phosphoadenosine 5'-phosphate. *Biochem. Biophys. Res. Commun.* **335,** 417–423
51. Kakuta, Y., Pedersen, L. G., Carter, C. W., Negishi, M. and Pedersen, L. C. (1997) Crystal structure of estrogen sulphotransferase. *Nat. Struct. Biol.* **4,** 904–908
52. Lee, K. A., Fuda, H., Lee, Y. C., Negishi, M., Strott, C. A., and Pedersen, L. C. (2003) Crystal structure of human cholesterol sulfotransferase (SULT2B1b) in the presence of pregnenolone and 3'-phosphoadenosine 5'-phosphate. Rationale for specificity differences between prototypical SULT2A1 and the SULT2BG1 isoforms. *J. Biol. Chem.* **278,** 44593–44599
53. Gamage, N. U., Tsvetanov, S., Duggleby, R. G., McManus, M. E., and Martin, J. L. (2005) The structure of human SULT1A1 crystallized with estradiol. An insight into active site plasticity and substrate inhibition with multi-ring substrates. *J. Biol. Chem.* **280**, 41482–41486

TABLE I

Primers used for generation of SULT1A1, SULT1A3 and SULT2A1 mutants[a].

Mutant		Primer
SULT1A1	F247A	5'-cccccaggag**gcc**atggaccaca-3'
SULT1A3	L247A	5'-cccccaggag**gcc**atggaccaca-3'
	L247F	5'-cccccaggag**ttc**atggaccaca-3'
	L247Y	5'-cccccaggag**tac**atggaccaca-3'
SULT2A1	M137C	5'-ctggaaaaac**tgc**aagtttatta-3'
	M137I	5'-ctggaaaaac**atc**aagtttatta-3'
	M137V	5'-ctggaaaaac**gtg**aagtttatta-3'
	M137K	5'-ctggaaaaac**aag**aagtttatta-3'
	M137W	5'-ctggaaaaac**tgg**aagtttatta-3'
	Y238A	5'-gagtgttgat**gct**gtagtggaca-3'
	Y238F	5'-gagtgttgat**ttt**gtagtggaca-3'
	Y238W	5'-gagtgttgat**tgg**gtagtggaca-3'

[a] Bold and underlined nucleotides indicate the designated positions for mutation. Only the sequence of the sense primer of each mutagenic set is shown.

TABLE II

RMSD values of SULT2A1/DHEA (1J99) and SULT2A1/PAP (1EFH) complex structures[a].

Residues			RMSD (Å)		
residues No.	1J99	1EFH	Backbone	Side chain	All atoms
4-230[b]	—	—	1.20	2.03	1.69
231	Tyr	Tyr	4.16	9.56	8.16
232	Ser	Ser	6.42	8.88	7.33
233	Leu	Leu	7.36	8.50	7.95
234	Leu	Leu	6.24	5.97	6.11
235	Ser	Ser	6.39	6.55	6.44
236	Val	Val	5.63	8.58	7.05
237	Asp	Asp	6.64	9.80	8.37
238	Tyr	Tyr	7.00	8.48	8.02
239	Val	Val	6.18	8.43	7.23
240	Val	Val	4.11	3.31	3.79
241	Asp	Asp	2.04	4.36	3.40
242	Lys	—[c]	—	—	—
243	Thr	—[c]	—	—	—
244	Gln	Gln	6.26	6.18	6.22
245	Leu	Leu	6.59	8.72	7.73
246	Leu	Leu	6.51	8.84	7.76
247	Arg	Arg	5.79	8.44	7.58
248	Lys	Lys	7.41	5.18	6.27
249	Gly	Gly	9.63	0	9.63
250	Val	Val	9.61	11.52	10.47
251	Ser	Ser	8.69	11.75	9.82
252	Gly	Gly	6.05	0	6.05
253-279[b]	—	—	0.98	2.34	1.83
Average			2.13	2.86	2.54

[a] Superposition of these two known structures was created by Combinatorial Extension (CE) (49) and the root-mean-square deviation (RMSD) was calculated by Swiss-Pdb Viewer (46).

[b] The average RMSD of these residues is less than 2.5 Å.

[c] Structure in this region was not solved.

TABLE III

Rate constants of SULT2A1 wild type and mutants using DHEA and ADT as substrates[a].

SULT2A1	DHEA				ADT			
	K_m	V_{max}	V_{max}/K_m	K_i	K_m	V_{max}	V_{max}/K_m	K_i
	μM	*nmole/min/mg*		μM	μM	*nmole/min/mg*		μM
Wild type	2.5 ± 0.7	227 ± 42	91	6.1 ± 1.7	1.4 ± 0.8	203 ± 86	145	0.7 ± 0.4
Y238A	3.3 ± 0.3	191 ± 8.3	58	45 ± 4.9	1.4 ± 0.1	55 ± 1.3	39	—[b]
Y238F	1.1 ± 0.2	108 ± 8.2	98	12 ± 1.7	1.5 ± 0.6	134 ± 38	90	2.2 ± 0.9
Y238W	0.7 ± 0.1	71 ± 5.1	101	15 ± 2.9	0.7 ± 0.6	79 ± 44	113	1.2 ± 0.8
M137I	1.3 ± 0.2	68 ± 4.9	52	36 ± 6.8	0.2 ± 0.06	42 ± 5.1	208	20 ± 7.9
M137V	1.9 ± 0.6	70 ± 8.9	37	53 ± 19	0.7 ± 0.3	60 ± 12	86	7.8 ± 3.2
M137W	1.3 ± 0.6	112 ± 32	86	7.1 ± 3.7	0.6 ± 0.2	61 ± 14	52	3.8 ± 1.6
M137K	ND[c]	ND[c]	ND[c]	ND[c]	ND[c]	ND[c]	ND[c]	ND[c]
M137I/Y238A	3.6 ± 0.7	48 ± 3.9	13	170 ± 53	1.4 ± 0.3	30 ± 1.8	22	159 ± 38
M137V/Y238A	6.5 ± 1.1	62 ± 4.0	9.5	466 ± 140	3.6 ± 0.4	37 ± 0.9	10	—[b]
M137W/Y238A	4.2 ± 0.3	97 ± 1.8	23	—[b]	2.0 ± 0.3	63 ± 2.2	31	—[b]
M137K/Y238A	ND[c]	ND[c]	ND[c]	ND[c]	ND[c]	ND[c]	ND[c]	ND[c]
V260E[d]	1.6 ± 0.4	160 ± 26	100	7.1 ± 1.9	1.4 ± 0.8	176 ± 74	126	1.2 ± 0.7
Y238A/V260E[d]	2.2 ± 0.1	144 ± 4.3	66	55 ± 4.8	1.8 ± 0.2	48 ± 1.4	27	—[b]

[a] Sulfotransferase activity was measured as indicated under "Experimental Procedures."

[b] Not applicable (substrate inhibition was not observed).

[c] Not determined due to undetectable or low level of activity.

[d] Monomer mutant of SULT2A1.

TABLE IV

RMSD of SULT2A1/DHEA (1J99) and SULT2A1/ADT (1OV4) complex structures.

Neighboring residues around DHEA within 5 Å				RMSD (Å)		
	residues No.	1J99	1OV4	Backbone	Side chain	All atoms
Alternative Orientation	14	Pro	Pro	0.24	0.18	0.22
	16	Met	Met	1.01	2.41	1.85
	17	Gly	Gly	0.61	0	0.61
	18	Phe	Phe	0.65	0.45	0.53
	43	Pro	Pro	0.28	0.29	0.29
	44	Lys	Lys	0.30	0.92	0.72
	47	Thr	Thr	0.30	0.32	0.31
	71	Ile	Ile	0.54	2.50	1.81
	72	Trp	Trp	0.68	0.68	0.68
	77	Trp	Trp	0.39	0.43	0.41
	80	Ser	Ser	0.31	0.55	0.41
	82	Ile	Ile	0.40	0.70	0.57
	99	His	His	0.18	0.23	0.21
	133	Phe	Phe	0.64	1.20	1.03
	134	Trp	Trp	0.45	0.30	0.35
	160	Tyr	Tyr	0.21	0.42	0.37
	231	Tyr	—[a]	—	—	—
	234	Leu	—[a]	—	—	—
Catalytic Orientation	14	Pro	Pro	0.24	0.18	0.22
	15	Thr	Thr	0.81	1.83	1.35
	16	Met	Met	1.01	2.41	1.85
	18	Phe	Phe	0.65	0.45	0.53
	44	Lys	Lys	0.30	0.92	0.72
	77	Trp	Trp	0.39	0.43	0.41
	99	His	His	0.18	0.23	0.21
	133	Phe	Phe	0.64	1.20	1.03
	134	Trp	Trp	0.45	0.30	0.35
	137	Met	Met	0.83	2.40	1.79
	138	Lys	Lys	0.91	1.62	1.35
	140	Leu	Leu	0.78	1.89	1.43
	231	Tyr	—[a]	—	—	—
	234	Leu	—[a]	—	—	—
	238	Tyr	Tyr	0.99	1.10	1.06

[a] Not solved in this region.

TABLE V

Dissociation constants of PAP, DHEA, and ADT in wild-type and mutated SULT2A1[a].

SULT2A1	Binary complex[b]	Ternary complex[c]	
	PAP	DHEA	ADT
	nM	*μM*	*μM*
Wild type	40.7 ± 8.2	0.8 ± 0.05	0.4 ± 0.04
Y238A	48.7 ± 8.6	6.9 ± 0.3	3.2 ± 0.1
M137I	44.2 ± 8.4	1.9 ± 0.3	0.4 ± 0.06
M137W	49.2 ± 7.8	0.6 ± 0.07	0.3 ± 0.03
M137I/Y238A	32.2 ± 7.3	7.2 ± 0.4	2.4 ± 0.4
M137W/Y238A	49.4 ± 8.1	3.7 ± 0.6	2.3 ± 0.4

[a] Dissociation constants were determined with spectrofluorimeter as indicated under "Experimental Procedures."

[b] The dissociation constants of binary complex was determined with PAP (5 to 365 nM) and SULT2A1 (100 nM).

[c] The dissociation constants of ternary complex were determined with DHEA (0.1 to 50 μM) or ADT (0.1 to 50 μM) and SULT2A1 (0.5 μM) in the presence of PAP (1 μM).

TABLE VI

Rate constants of SULT1A1, SULT1A3 and their mutants[a].

Enzyme		Substrate	K_m	V_{max}	V_{max}/K_m	K_i
			μM	*nmole/min/mg*		*uM*
SULT1A1	Wild type	*p*-Nitrophenol	2.2 ± 1.0	323 ± 116	147	0.8 ± 0.4
	F247A		3.2 ± 0.8	1437 ± 217	449	9.4 ± 2.1
SULT1A3	Wild type		6.8 ± 0.9	623 ± 30	92	174 ± 23
	L247A	Dopamine	22 ± 1.2	1149 ± 32	52	282 ± 22
	L247Y		36 ± 14	1669 ± 457	46	61 ± 26

[a] Sulfotransferase activity was measured as indicated under "Experimental Procedures."

Figure 1. Sequence alignment of some cytosolic sulfotransferases. The PSB and PB loop that interacted with the 5'-phosphate of PAP and the residues involved in binding the 3'-phosphate of PAP were shown with a *cyan* background. The other significant residues reported in previous researches were shown in *pink* background. They are as follows: Ser-134 in rat SULT1A1 (9), His-108 in mouse SULT1E1 (10), Tyr-81 in mouse SULT1E1 (11), Glu-146 in human SULT1A3 (12), Asp-86 in human SULT1A3 (13-14), KTVE motif among

most cytosolic sulfotransferase (15), Cys-66 and Cys-232 in rat SULT1A1 (16), and Phe-247 in human SULT1A1 (17). Met-137 and Tyr-238 of SULT2A1 reported in this study were indicated by a *red* star. The multiple sequence alignment was generated by ClustalW (18).

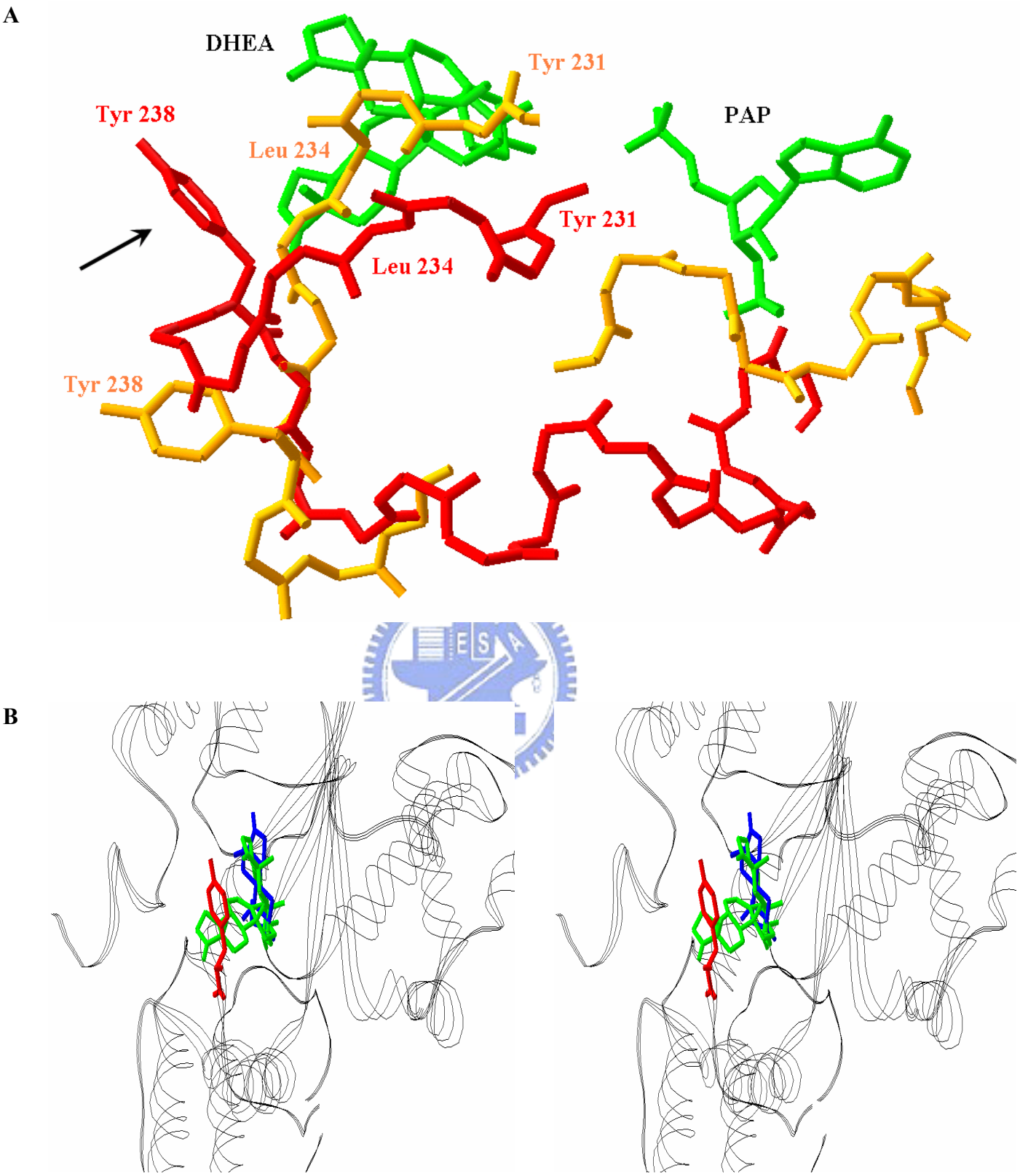

Figure 2. Structures of the loop from residues Tyr-231 to Gly-252 of SULT2A1/PAP, SULT2A1/DHEA and SULT2A1/ADT complexes. *A*. Loop and substrate binding site.

Superposition of this loop was performed between the SULT2A1/PAP (*orange*) and SULT2A1/DHEA (*red*) complex structures. The structure of SULT2A1/ADT at this region is very similar to that of SULT2A1/DHEA. The two ligands were colored in *green* and the proposed entrance of substrate was marked by an arrow. *B*. Stereoview of the SULT2A1/DHEA and the SULT2A1/ADT complex structures. Tyr-238 (*red*) acted as a gate residue for the substrate-binding site. The DHEA molecule was placed in two orientations and was colored in *green*; ADT molecule was colored in *blue*.

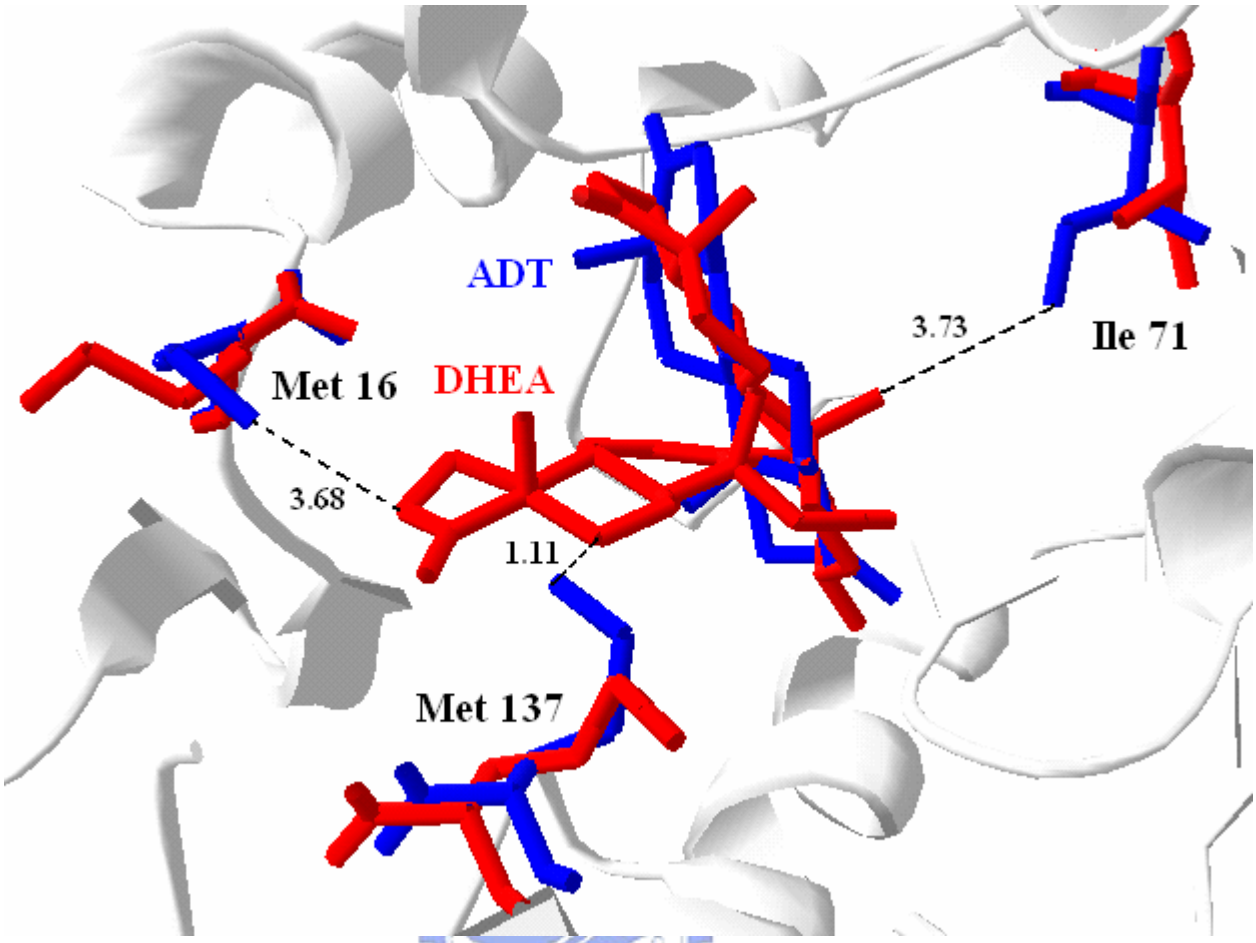

Figure 3. Binding modes of DHEA and ADT molecules in SULT2A1. Comparison of the binding mode was performed between the SULT2A1/DHEA (*red*) and the SULT2A1/ADT (*blue*) complex structures. The residues Met-16, Ile-71 and Met-137 around the DHEA and ADT molecules were shown. DHEA showed van der Waals interactions (shown by *dotted lines*) with Met-16, Ile-71 and Met-137 with C-16, C-19 and C-12 of DHEA, respectively.

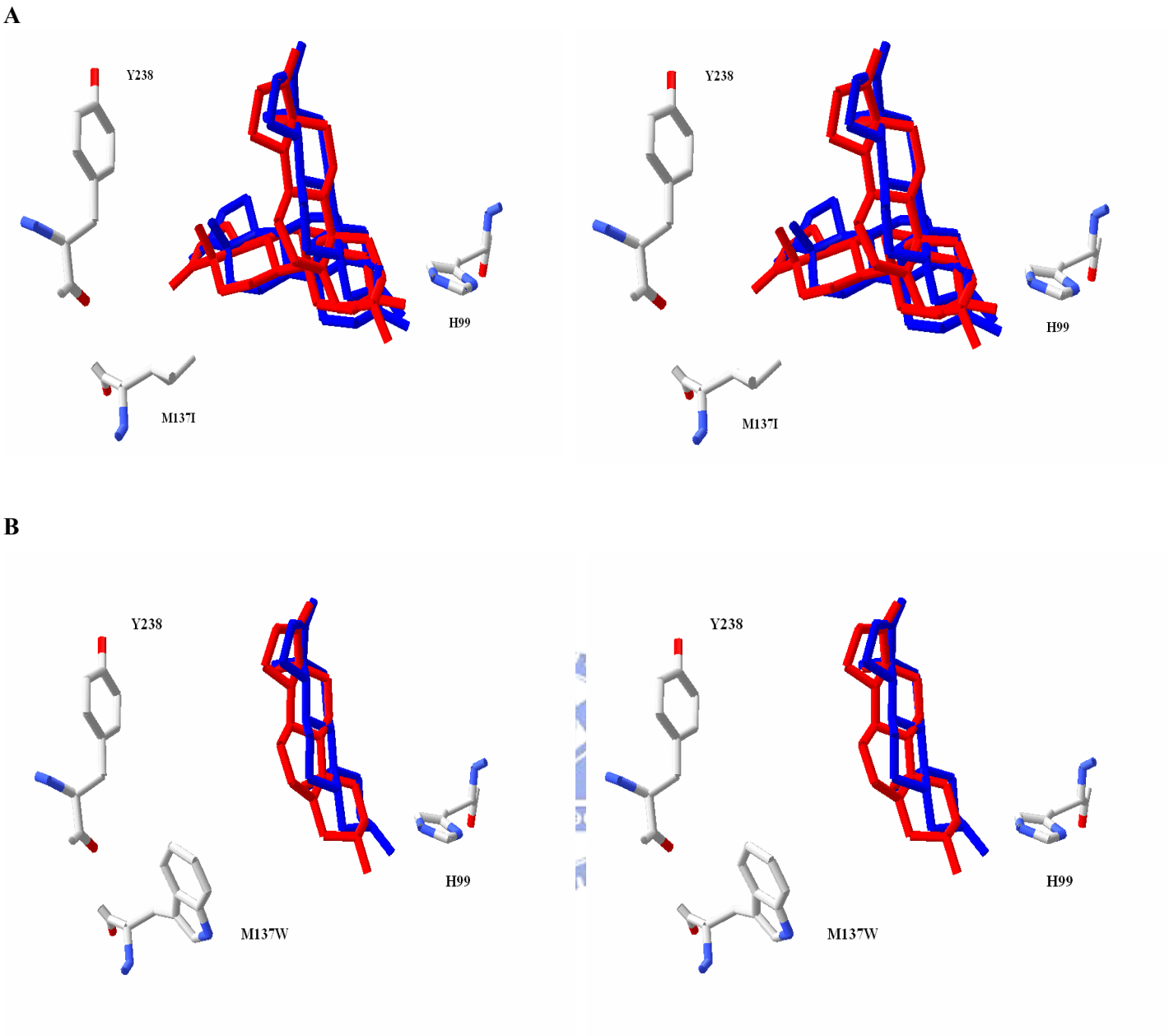

Figure 4. Molecular modeling of DHEA and ADT in M137I or M137W of SULT2A1. Homology modeling of the *A*. M137I and *B*. M137W were constructed using the SWISS-MODEL server based on the SULT2A1/DHEA complex structure (PDB code: 1J99) (37). These modeled structures were used in GOLD as templates to dock DHEA (*red*) and ADT (*blue*) molecules.

A

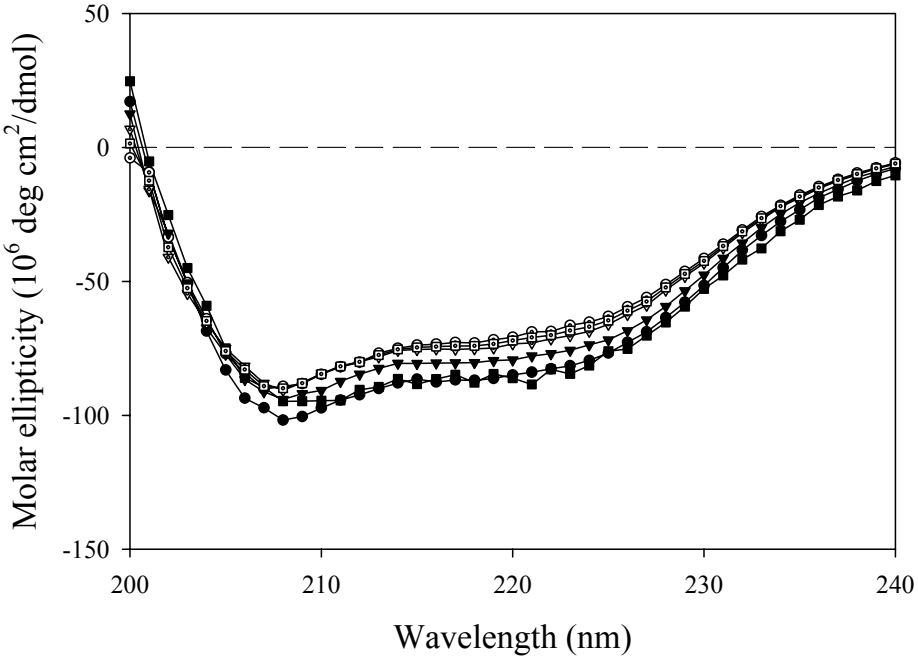

B

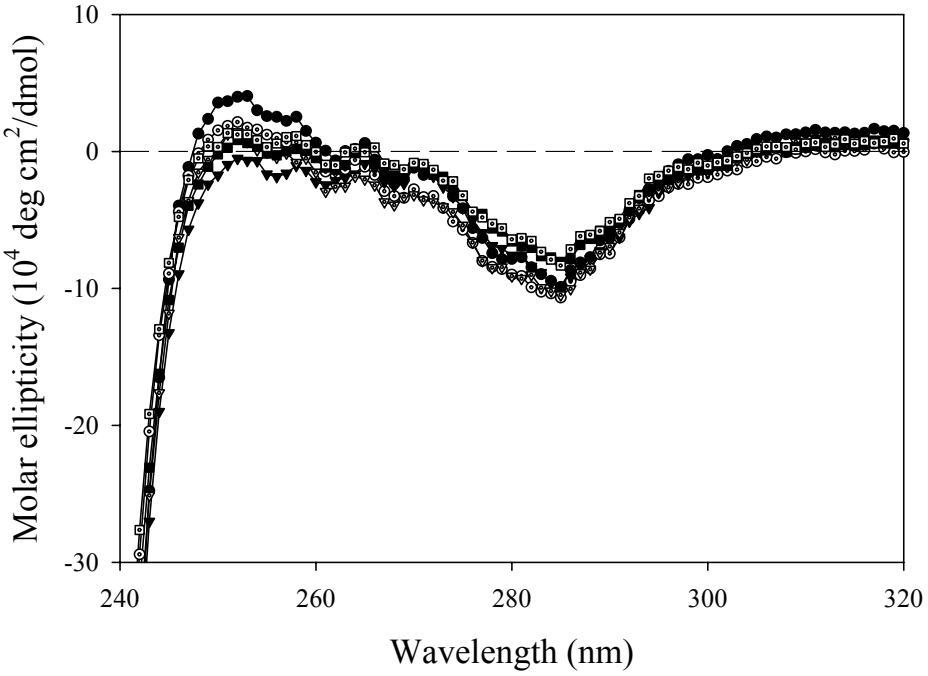

Figure 5. Circular dichroism specrtra of wild-type and mutated SULT2A1. CD measurements were carried out on a Jasco J715 spectropolarimeter and processed data with J-700 standard analysis version 1.33.00 (Jasco, Japan). CD spectra of enzymes at a concentration of 7.4 μM (*A*) and 4 μM (*B*) in 20 mM phosphate buffer (pH 7.0) were

measured in a 1 cm light path length quartz cell in the near-UV range (240-320 nm) and 1 mm light path in the far-UV (200-240 nm) at room temperature individually. The white symbols were the mutants while Tyr-238 was mutated to alanine, and the circle, inverted triangle, square symbols were wild type, M137I, and M137W, respectively.

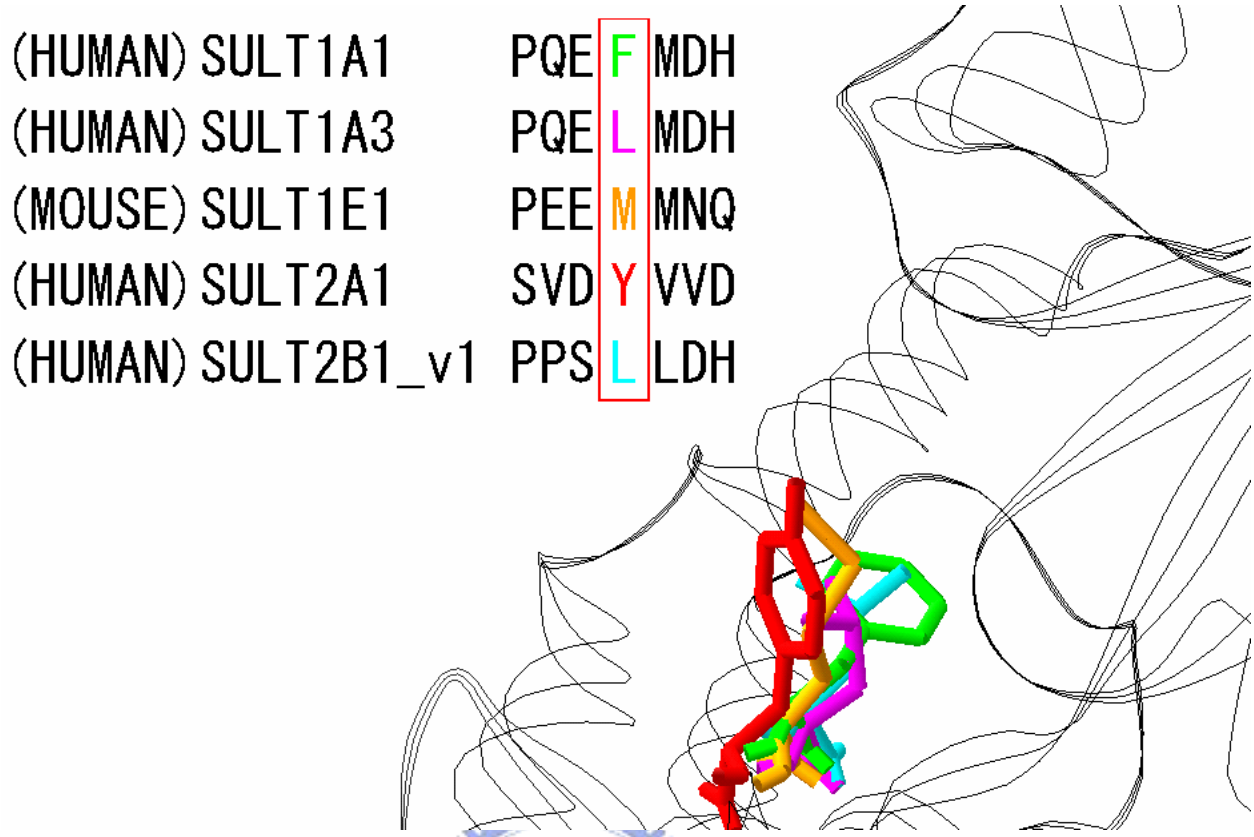

Figure 6. Multiple sequence and structure alignment of Tyr-238 corresponding residues among some solved-structure sulfotransferases. The in-position residues of Tyr-238 (*red*) of SULT2A1 were Phe-247 (*green*) of human SULT1A1, Leu-247 (*magenta*) of human SULT1A3, Met-247 (*orange*) of mouse SULT1E1, Leu-249 (*cyan*) of human SULT2B1_v1. Superposition of these known-structure sulfotransferases was created by Combinatorial Extension (CE) (49), and the multiple sequence alignment was produced by ClustalW (18).

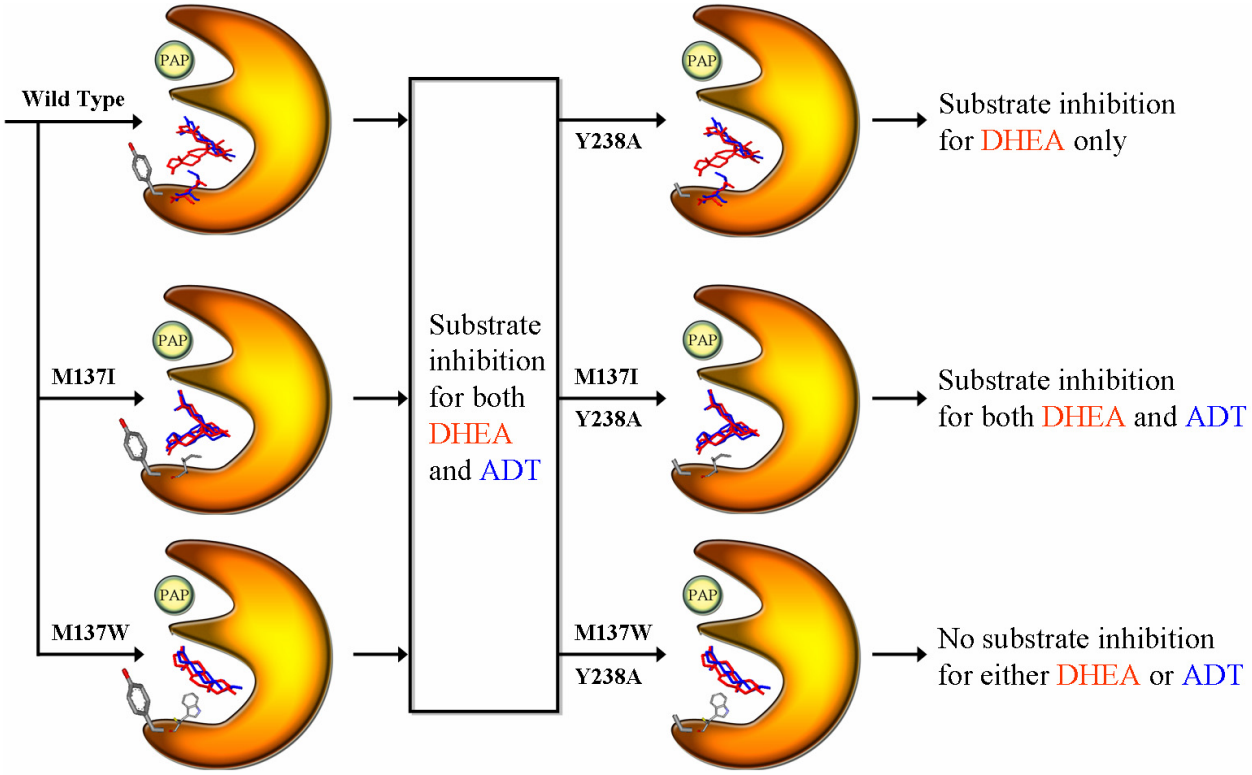

Figure 7. Schematic illustration of SULT2A1 substrate binding orientation and inhibition modulated by Met-137 and Tyr-238. The ternary dead-end complex was conceived of presence with PAP, DHEA or ADT simultaneously. The DHEA (*red*) and ADT (*blue*) compound structures were shown as described before and the substrate binding orientations of SULT2A1 were regulated by M137I and M137W in wild type SULT2A1 was colored in *red* (SULT2A1/DHEA) and *blue* (SULT2A1/ADT), respectively. The Met-137 and Tyr-238 were mutated to demonstrate their effects on the substrate binding orientation and inhibition schematically.

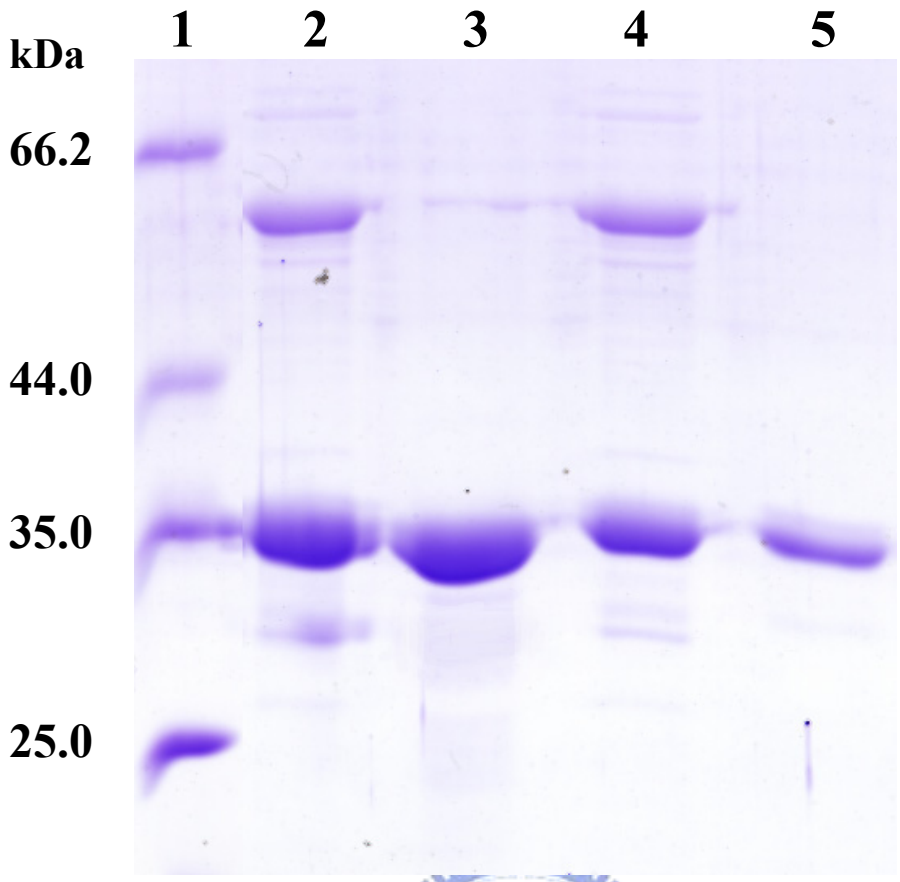

Figure 8. SDS-PAGE analysis of M137I and M137W. Lane 1 was protein marker consisted of bovine serum albumin (66.2 kDa), ovalbumin (44 kDa), lactate dehydrogenase (35 kDa), and restriction endonuclease Bsp98I (25 kDa). Lane 2 and lane 4 are M137I and M137W, respectively, and eluted from GSTrap chromatography. Lane 3 and lane 5 are M137I and M137W, respectively, and eluted from Q sepharose.

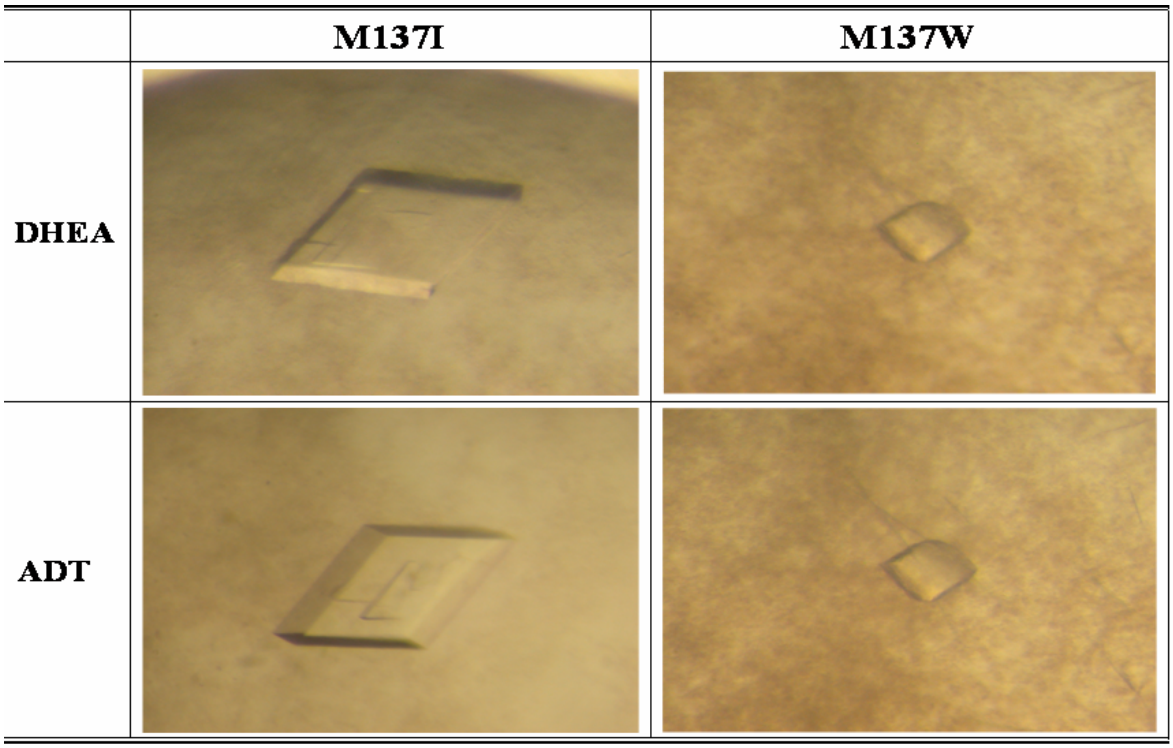

Figure 9. M137I and M137W mutants cocrystallized with DHEA and ADT. These crystals were obtained in a hanging drop method by vapor diffusion. Equal volumes of enzyme stock at 10 mg ml^{-1} were mixed with the reservoir solution containing 100 mM HEPES (pH 7.5), 100mM NaCl, and 1.6 M $(NH_4)_2SO_4$. The crystals appeared in 2 ± 3 days and grew to dimensions after 7 ± 10 days.

APPENDIX

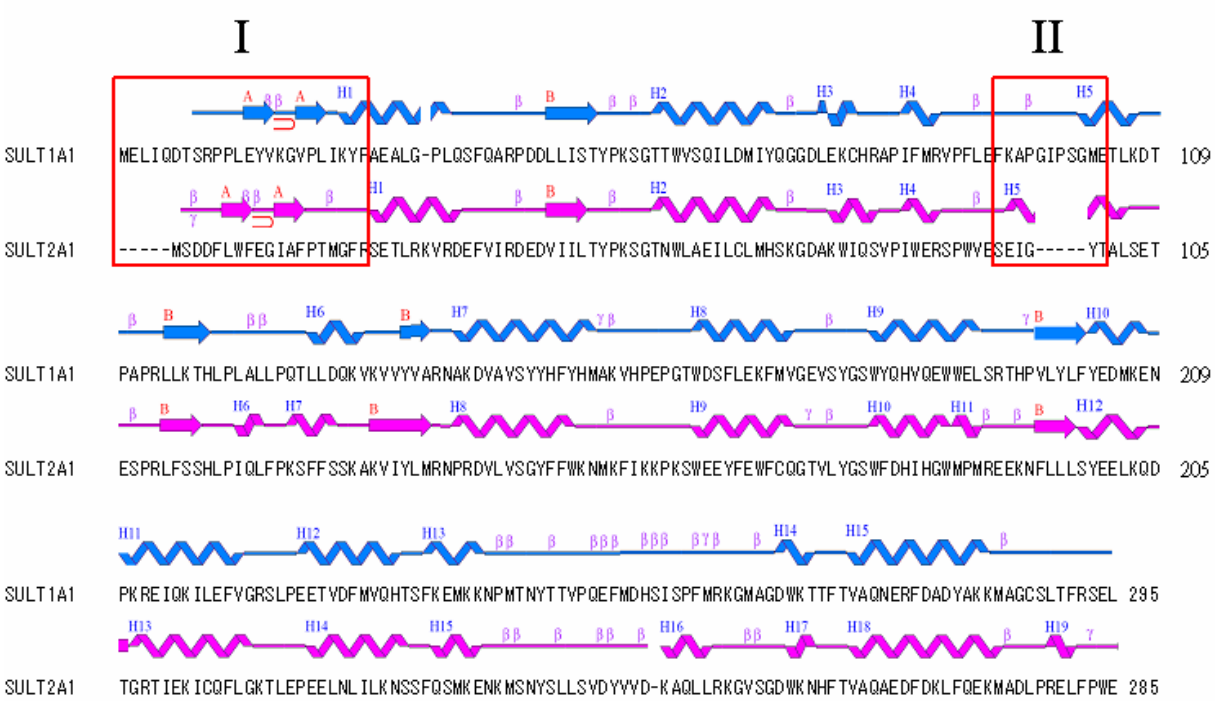

A1. Primary and secondary structural alignment between SULT1A1 and SULT2A1. The pairwise sequence alignment was produced by ClustalW. The secondary structures of SULT1A1 and SULT2A1 were colored in *cyan* and *pink*, respectively. The putative substrate specificity loops were boxed in *red*.

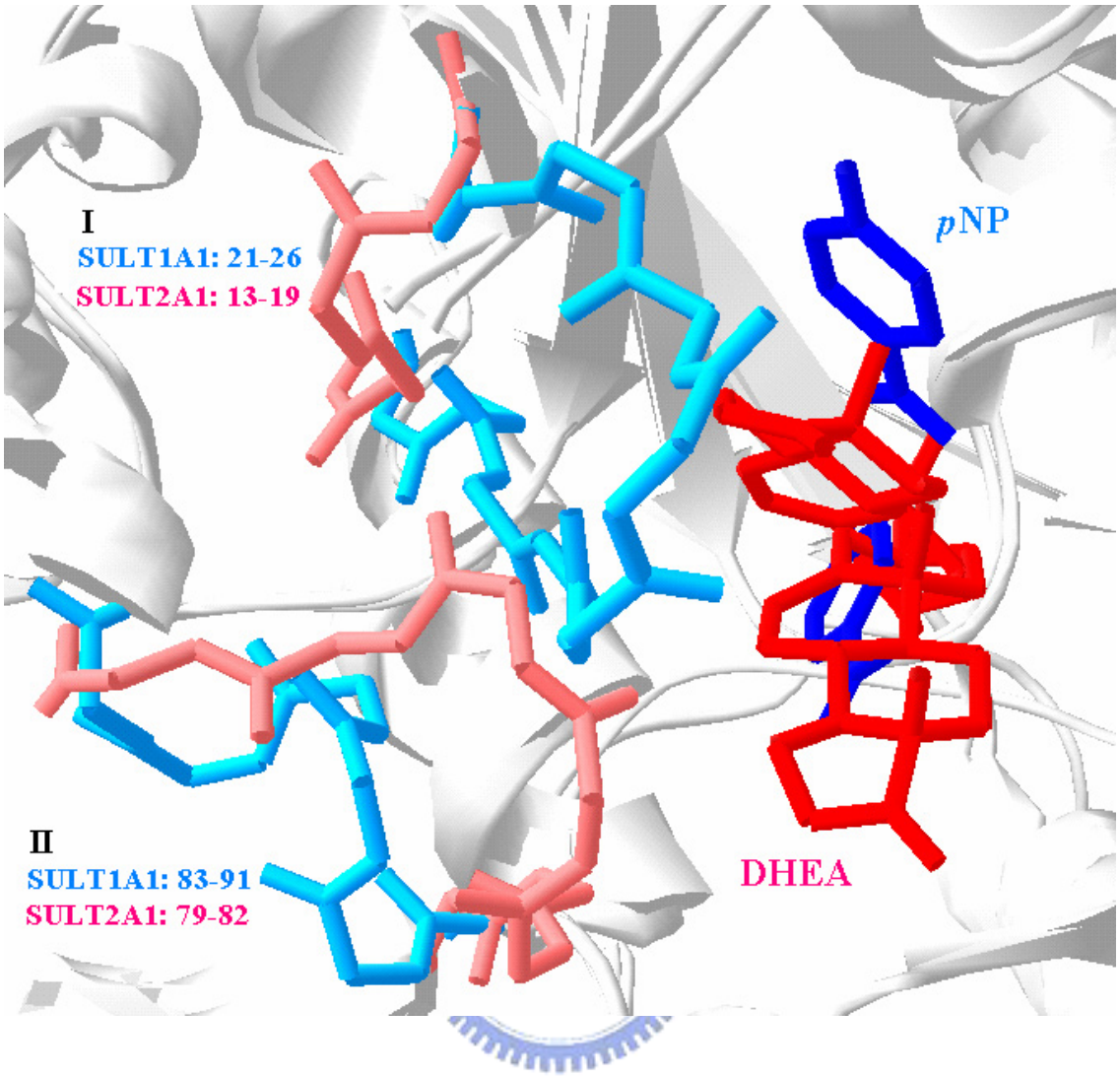

A2. Tertiary structural alignment between SULT1A1 and SULT2A1. The loop I and loop II of SULT1A1 (*cyan*) and SULT2A1 (*pink*) were shown and the substrates of *p*NP for SULT1A1 and DHEA for SULT2A1 were colored in *blue* and *red*, respectively. Structural superimposition of SULT1A1 and SULT2A1 was created by Swiss-Pdb Viewer.

CLUSTAL W (1.82) multiple sequence alignment (within 6 Å)

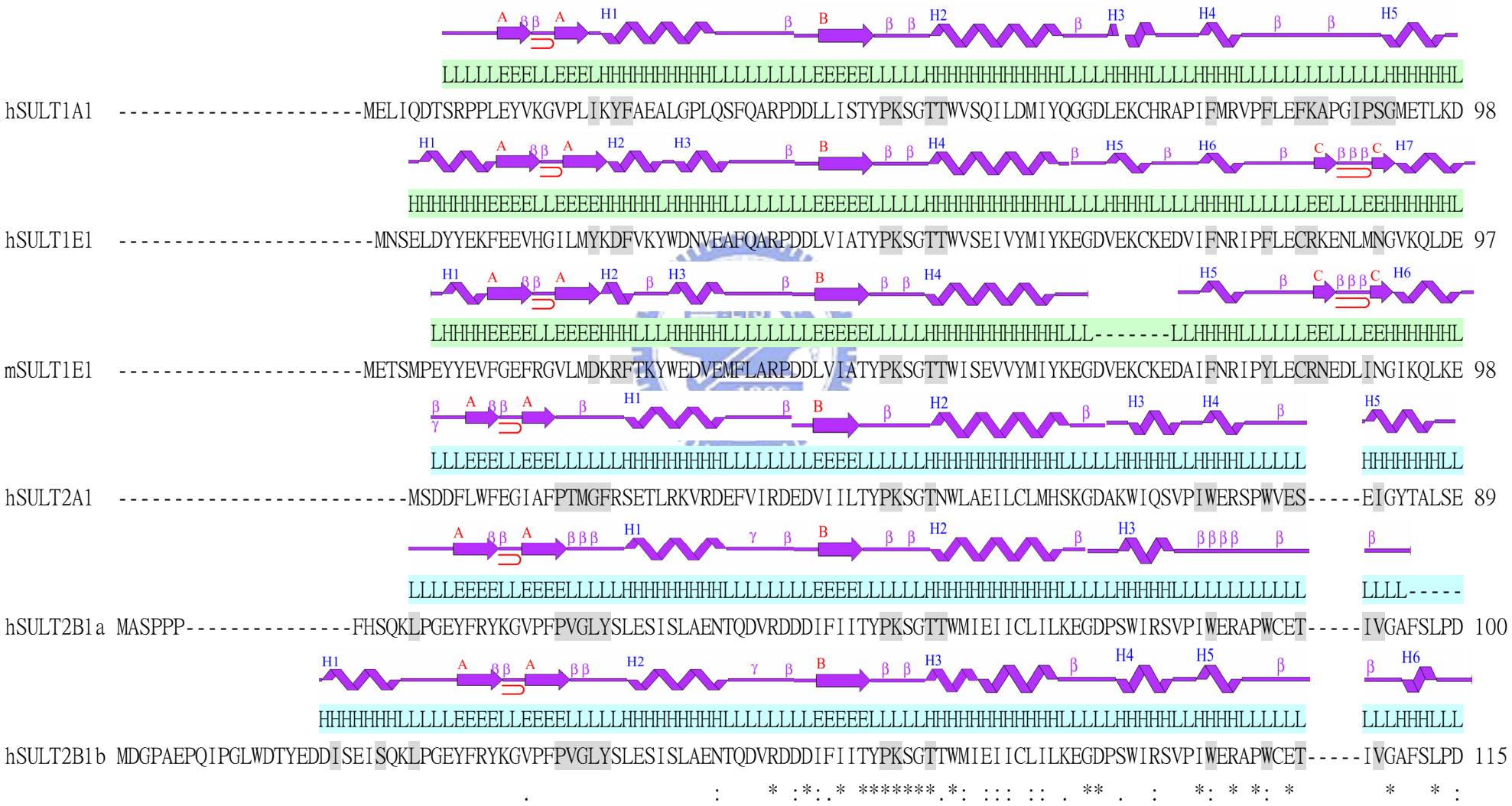

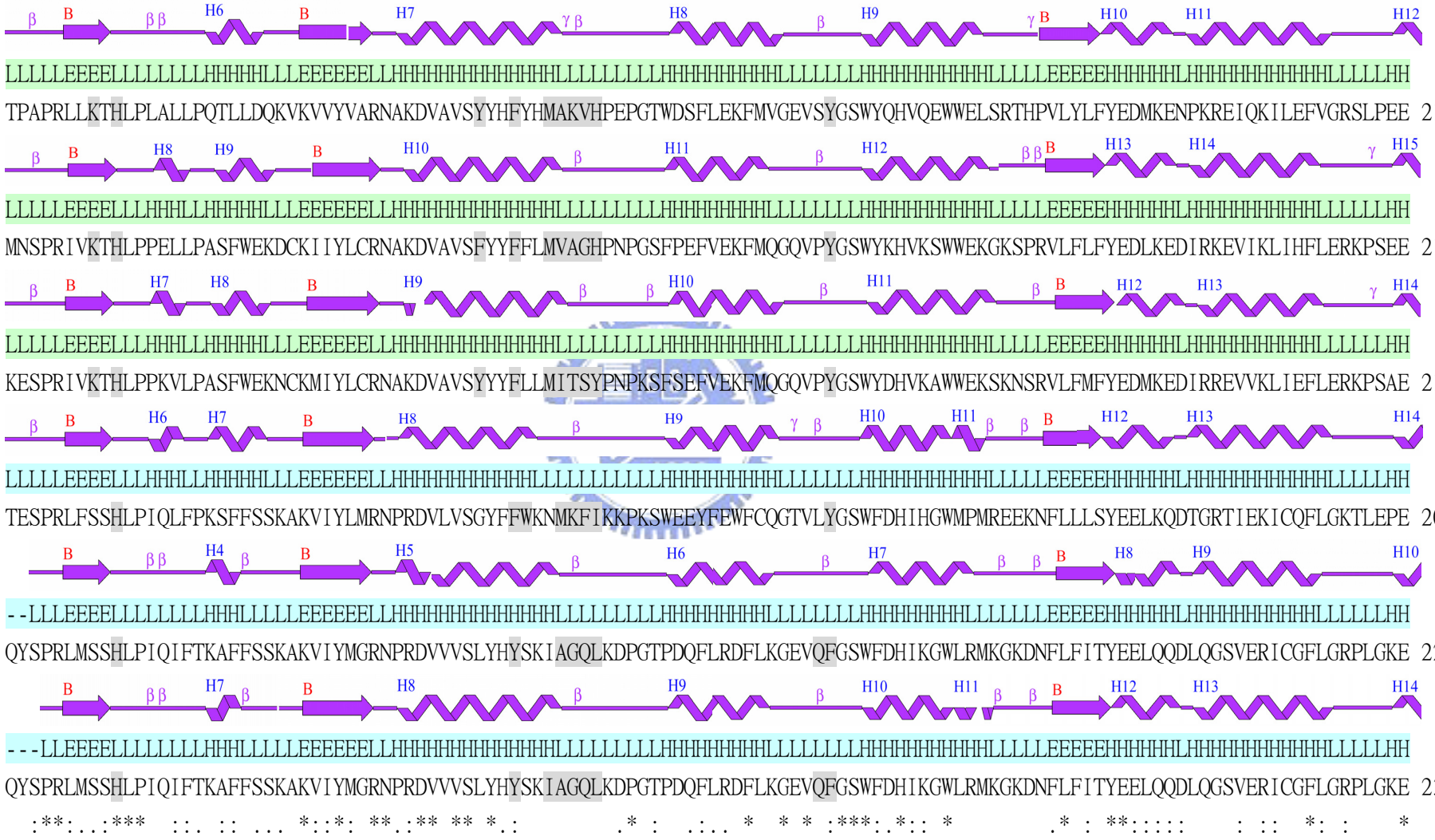
β B ββ H6 B H7 γβ H8 β H9 γ B H10 H11 H12
LLLLLEEEELLLLLLLLHHHHHLLLEEEEEELLHHHHHHHHHHHHHHHLLLLLLLLLLHHHHHHHHHHLLLLLLLHHHHHHHHHHHLLLLLEEEEEHHHHHHLHHHHHHHHHHHLLLLLHH
hSULT1A1 TPAPRLLKTHLPLALLPQTLLDQKVKVVYVARNAKDVAVSYYHFYHMAKVHPEPGTWDSFLEKFMVGEVSYGSWYQHVQEWWELSRTHPVLYLFYEDMKENPKREIQKILEFVGRSLPEE 218
β B H8 H9 B H10 β H11 β H12 ββ B H13 H14 γ H15
LLLLLEEEELLLHHHLLHHHHHLLLEEEEEELLHHHHHHHHHHHHHHHLLLLLLLLLLHHHHHHHHHHLLLLLLLLHHHHHHHHHHHLLLLLEEEEEHHHHHHLHHHHHHHHHHHLLLLLLHH
hSULT1E1 MNSPRIVKTHLPPELLPASFWEKDCKIIYLCRNAKDVAVSFYYFFLMVAGHPNPGSFPEFVEKFMQGQVPYGSWYKHVKSWWEKGKSPRVLFLFYEDLKEDIRKEVIKLIHFLERKPSEE 217
β B H7 H8 B H9 β β H10 β H11 β B H12 H13 γ H14
LLLLLEEEELLLHHHLLHHHHHLLLEEEEEELLHHHHHHHHHHHHHHHLLLLLLLLLLHHHHHHHHHHLLLLLLLLHHHHHHHHHHHLLLLLEEEEEHHHHHHLHHHHHHHHHHHLLLLLLHH
mSULT1E1 KESPRIVKTHLPPKVLPASFWEKNCKMIYLCRNAKDVAVSYYYFLLMITSYPNPKSFSEFVEKFMQGQVPYGSWYDHVKAWWEKSKNSRVLFMFYEDMKEDIRREVVKLIEFLERKPSAE 218
β B H6 H7 B H8 β H9 γ β H10 H11 β β B H12 H13 H14
LLLLLEEEELLLHHHLLHHHHHLLLEEEEEELLHHHHHHHHHHHHHHHLLLLLLLLLLHHHHHHHHHHLLLLLLLLHHHHHHHHHHHLLLLLEEEEEHHHHHHLHHHHHHHHHHHLLLLLLHH
hSULT2A1 TESPRLFSSHLPIQLFPKSFFSSKAKVIYLMRNPRDVLVSGYFFWKNMKFIKKPKSWEEYFEWFCQGTVLYGSWFDHIHGWMPMREEKNFLLLSYEELKQDTGRTIEKICQFLGKTLEPE 209
B ββ H4 β B H5 β H6 β H7 β β B H8 H9 H10
--LLLEEEELLLLLLLLHHHLLLLLEEEEEELLHHHHHHHHHHHHHHHLLLLLLLLLLHHHHHHHHHHLLLLLLLLHHHHHHHHHHHLLLLLLLEEEEEHHHHHHLHHHHHHHHHHHLLLLLLHH
hSULT2B1a QYSPRLMSSHLPIQIFTKAFFSSKAKVIYMGRNPRDVVVSLYHYSKIAGQLKDPGTPDQFLRDFLKGEVQFGSWFDHIKGWLRMKGKDNFLFITYEELQQDLQGSVERICGFLGRPLGKE 220
B ββ H7 β B H8 β H9 β H10 H11 β β B H12 H13 H14
---LLEEEELLLLLLLLHHHLLLLLEEEEEELLHHHHHHHHHHHHHHHLLLLLLLLLLHHHHHHHHHHLLLLLLLLHHHHHHHHHHHLLLLLLLEEEEEHHHHHHLHHHHHHHHHHHLLLLLLHH
hSULT2B1b QYSPRLMSSHLPIQIFTKAFFSSKAKVIYMGRNPRDVVVSLYHYSKIAGQLKDPGTPDQFLRDFLKGEVQFGSWFDHIKGWLRMKGKDNFLFITYEELQQDLQGSVERICGFLGRPLGKE 235
:**:..:*** :: :: ... *::*: **.:** ** *.: .* : .:.. * * * :***:.*:: * .* : **::::: : :: *: : *

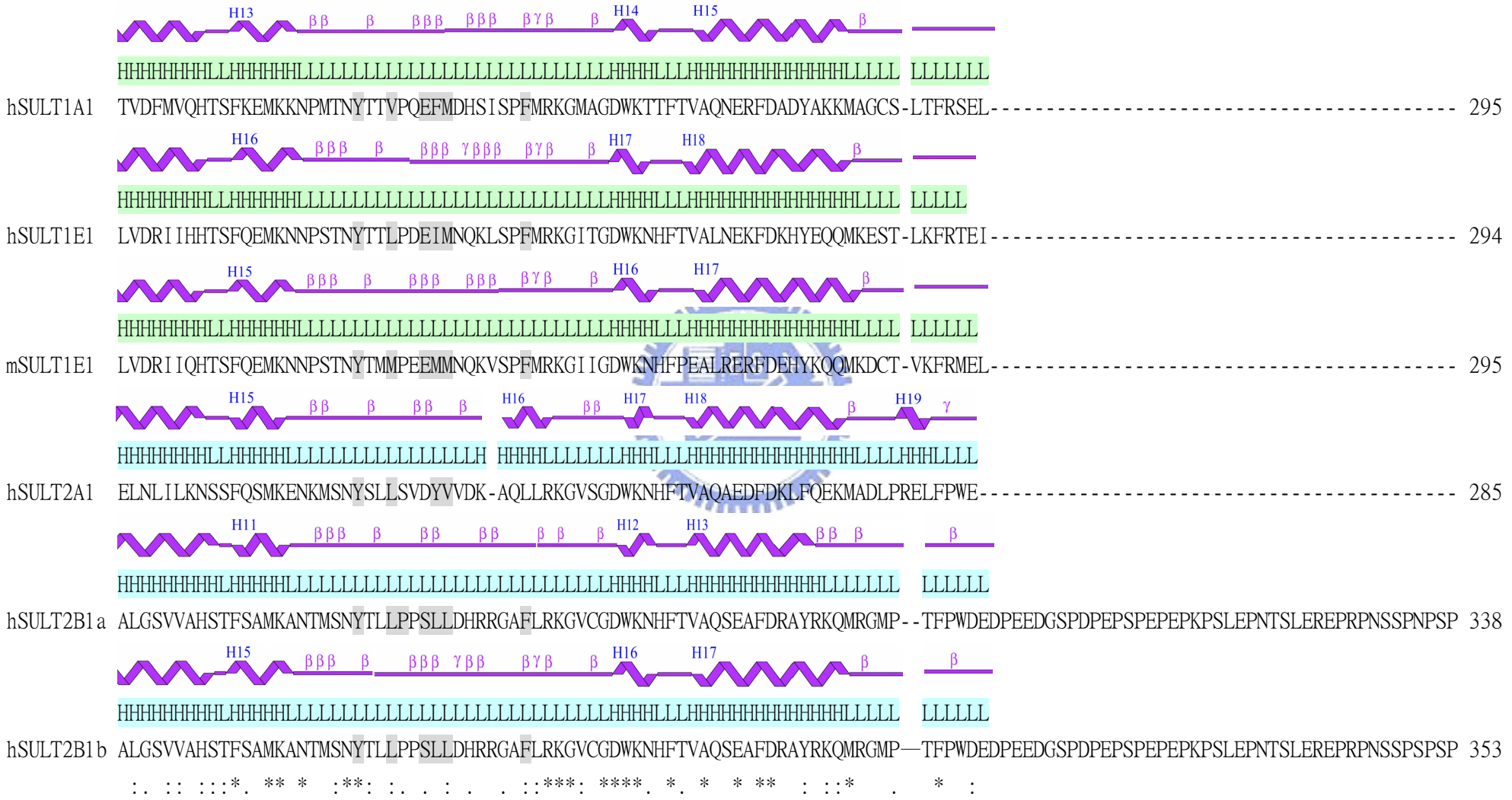
H13 ββ β βββ βββ βγβ β H14 H15 β
HHHHHHHHLLHHHHHHLLLLLLLLLLLLLLLLLLLLLLLLLLLLLLHHHHLLLHHHHHHHHHHHHHLLLLL LLLLLLL
hSULT1A1 TVDFMVQHTSFKEMKKNPMTNYTTVPQEFMDHSISPFMRKGMAGDWKTTFTVAQNERFDADYAKKMAGCS-LTFRSEL---------- 295
H16 βββ β βββ γβββ βγβ β H17 H18 β
HHHHHHHHLLHHHHHHLLLLLLLLLLLLLLLLLLLLLLLLLLLLLLHHHHLLLHHHHHHHHHHHHHLLLL LLLLL
hSULT1E1 LVDRIIHHTSFQEMKNNPSTNYTTLPDEIMNQKLSPFMRKGITGDWKNHFTVALNEKFDKHYEQQMKEST-LKFRTEI---------- 294
H15 βββ β βββ βββ βγβ β H16 H17 β
HHHHHHHHLLHHHHHHLLLLLLLLLLLLLLLLLLLLLLLLLLLLLLHHHHLLLHHHHHHHHHHHHHLLLL LLLLLL
mSULT1E1 LVDRIIQHTSFQEMKNNPSTNYTMMPEEMMNQKVSPFMRKGIIGDWKNHFPEALRERFDEHYKQQMKDCT-VKFRMEL---------- 295
H15 ββ β ββ β H16 ββ H17 H18 β H19 γ
HHHHHHHHLLHHHHHLLLLLLLLLLLLLLLLLLH HHHHLLLLLLLLHHHLLLHHHHHHHHHHHHHHLLLLHHHLLLL
hSULT2A1 ELNLILKNSSFQSMKENKMSNYSLLSVDYVVDK-AQLLRKGVSGDWKNHFTVAQAEDFDKLFQEKMADLPRELFPWE---------- 285
H11 βββ β ββ ββ β β β H12 H13 ββ β β
HHHHHHHHHLHHHHHLLLLLLLLLLLLLLLLLLLLLLLLLLLLLLHHHHLLLHHHHHHHHHHHHLLLLLLL LLLLLL
hSULT2B1a ALGSVVAHSTFSAMKANTMSNYTLLPPSLLDHRRGAFLRKGVCGDWKNHFTVAQSEAFDRAYRKQMRGMP--TFPWDEDPEEDGSPDPEPSPEPEPKPSLEPNTSLEREPRPNSSPNPSP 338
H15 βββ β βββ γββ βγβ β H16 H17 β β
HHHHHHHHHLHHHHHLLLLLLLLLLLLLLLLLLLLLLLLLLLLLLHHHHLLLHHHHHHHHHHHHHLLLLL LLLLLL
hSULT2B1b ALGSVVAHSTFSAMKANTMSNYTLLPPSLLDHRRGAFLRKGVCGDWKNHFTVAQSEAFDRAYRKQMRGMP—TFPWDEDPEEDGSPDPEPSPEPEPKPSLEPNTSLEREPRPNSSPSPSP 353
:. :: :::*. ** * :**: :. . : . . ::***: ****. *. * * ** : ::* . * :

A3. Multiple primary and secondary structural alignment of partial cytosolic sulfotransferases. The cytosolic sulfotransferases could divide into two families: SULT1 and SULT2. The SULT1 included human SULT1A1, human SULT1E1, and mouse SULT1E1. Furthermore, SULT2 was consisted of human SULT2A1, human SULT2B1_v1, and SULT2B1_v2. The amino acid sequence alignment was produced by ClustalW. The secondary structures of SULT1 and SULT2 were colored in *green* and *blue*, respectively. The secondary structures helix, sheet, and loop were abbreviated to H, E, and L individually. The residues within the 6 Å around the substrate were highlighted in the *gray* background.

Autobiography

2004-2006: Department of Biological Science and Technology and Institute of Biochemical Engineering, National Chiao Tung University, Hsinchu, Taiwan, ROC

（國立交通大學生物科技研究所）

2000-2004: Department of Applied Chemistry, National Chiao Tung University, Hsinchu, Taiwan, ROC

（國立交通大學應用化學系）

1997-2000: National Pan Chiao Senior High School

（國立板橋高級中學）